AD-A159 122 RESEARCH ON MATERIALS AND COMPONENTS FOR OPTO-ELECTRONIC SIGNAL PROCESSIN..(U) CALIFORNIA UNIV SAN DIEGO LA JOLLA DEPT OF ELECTRICAL ENGINEE.. 1/1

UNCLASSIFIED W S CHANG ET AL. 01 OCT 84 AFOSR-TR-85-0659 F/G 20/6 NL

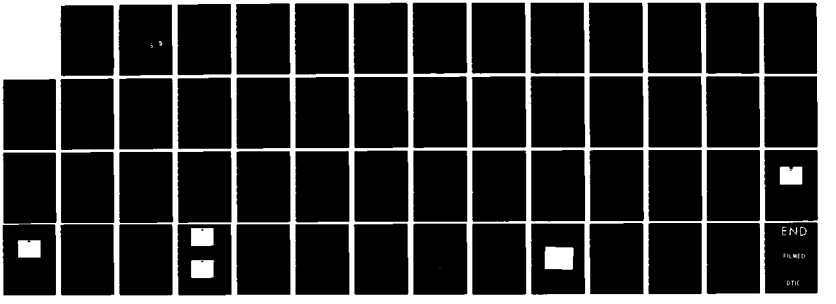

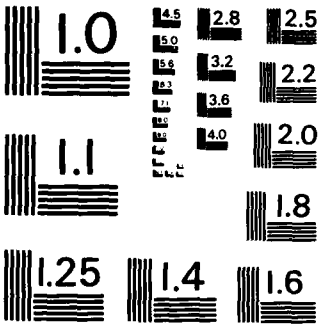

MICROCOPY RESOLUTION TEST CHART
NATIONAL BUREAU OF STANDARDS-1963-A

SECURITY CLASSIFICATION OF THIS PAGE (When Data Entered)

REPORT DOCUMENTATION PAGE

1. REPORT NUMBER: AFOSR-TR- 85-0659

AD-A159 122

2. GOVT ACCESSION NO.

3. RECIPIENT'S CATALOG NUMBER

4. TITLE (and Subtitle)

~~Properties of Chirped Grating Lenses in Optical Waveguides~~ Use title on title page

5. TYPE OF REPORT & PERIOD COVERED

Final Scientific Report
10Oct79 - 30Sep84

6. PERFORMING ORG. REPORT NUMBER

7. AUTHOR(s)

William S. C. Chang, Jean-Marc Delavaux, Siamak Forouhar, C. C. Sun, Timothy Van Eck and H. H. Wieder

8. CONTRACT OR GRANT NUMBER(s)

AFOSR-80-0037

9. PERFORMING ORGANIZATION NAME AND ADDRESS

Dept. of Electrical Engineering & Computer Sciences
University of California, San Diego
La Jolla, CA 92093

10. PROGRAM ELEMENT, PROJECT, TASK AREA & WORK UNIT NUMBERS

61102F
2305/B1

11. CONTROLLING OFFICE NAME AND ADDRESS

12. REPORT DATE

October 1st, 1984

13. NUMBER OF PAGES

51

14. MONITORING AGENCY NAME & ADDRESS (if different from Controlling Office)

Col. Robert Carter
AFOSR/NE, Bolling Air Force Base
Washington, DC 20332

15. SECURITY CLASS. (of this report)

unclassified

15a. DECLASSIFICATION/DOWNGRADING SCHEDULE

16. DISTRIBUTION STATEMENT (of this Report)

Approved for public release; distribution unlimited.

17. DISTRIBUTION STATEMENT (of the abstract entered in Block 20, if different from Report)

DTIC ELECTE SEP 12 1985 S D E

18. SUPPLEMENTARY NOTES

19. KEY WORDS (Continue on reverse side if necessary and identify by block number)

Chirped grating, waveguide lens, opto-electronic signal processing, electrorefraction III-V compound opto-electronic devices

20. ABSTRACT (Continue on reverse side if necessary and identify by block number)

Design of chirped grating lenses on optical waveguides for opto-electronic signal processing is presented in this report. Fundamental limitations of the performance of chirped grating lenses due to material properties, fabrication tolerance and design parameters are discussed. In addition electro-absorption and electro-refraction properties in GaAs and InP semiconductors are presented. Cross modulation of optical radiations at two different wavelengths has been observed in GaAs. It has the potential of exhibiting optical AND logic.

DD FORM 1 JAN 73 1473 EDITION OF 1 NOV 65 IS OBSOLETE

SECURITY CLASSIFICATION OF THIS PAGE (When Data Entered)

FINAL SCIENTIFIC REPORT

Research on Materials and Components for Opto-Electronic Signal Processing

Sponsored by
Air Force Office of Scientific Research
Air Force Systems Command, USAF
under AFOSR Grant No. 80-0037
October 1st, 1979 through September 30th, 1984

submitted by
William S. C. Chang (Principal Investigator)
Jean-Marc Delavaux, Siamak Forouhar
C. C. Sun, Timothy Van Eck, L. M. Walpita
Christopher Warren and H. H. Wieder

Department of Electrical Engineering and Computer Sciences
C-014
University of California, San Diego
La Jolla
California 92093
Tel: (619) 452-2737

1. Introduction

For signal processing in planar waveguides, it is necessary to integrate, focus, collimate, image or Fourier-analyze guided wave beams by efficient and low cost lenses that have diffraction-limited performance and low noise. The investigation of chirped grating lenses as shown in Figure 1 has been the principal task of this research program until September 1982. During FY 1983 the research effort on the $LiNbO_3$ waveguide lens has been shifted partially to a new applied research program awarded jointly to the TRW Electro-optic Research Center and the University of California, San Diego (UCSD) under the sponsorship of the Air Force Avionics Laboratory, Wright Patterson Air Force Base, Contract No. F33615-82-C-1751, entitled "Optical Waveguide Diffraction Elements". Only the research concerning the fundamental limitations of the chirped grating lenses had remained in this contract. During FY 1984 all the research on lenses had been shifted to the joint TRW-UCSD program. We consider this as a technology transfer process. In this process, the original work was carried out under the basic research (6.1) program sponsored by AFOSR, the development of prototype lenses were carried out under the applied research (6.2) program jointly by the University and industry. No research on chirped grating lenses will be carried out at UCSD after 1984. TRW will be completely responsible for any further development work in the future. In section 2, we will summarize all the research accomplishments on chirped grating lenses at UCSD. The technical details of chirped grating lenses are contained in the 12 papers published in the open literature; they are also summarized in the AFOSR Scientific Report entitled "Properties of Chirped Grating Lenses in Optical Waveguides", October 1st, 1984.

In the meantime, a new materials and device research program on the investigation of the electro-optical effects of III-V compound semiconductor materials and devices near their bandgap has been initiated in FY 1983. It has been recognized for some time that optical signal processing holds considerable promise for high speed signal processing in DOD applications due to its parallel processing capabilities. In addition, optical signals also need to be switched, processed, multiplexed, and demultiplexed in optical fiber communications. However, characteristics of the materials and components (including microfabrication processing technology) must be improved before the full potential of combined opto-electronic signal processing can be realized. In III-V compound semiconductors, optical devices such as lasers and detectors have already been realized and used in many applications including optical fiber communications. Electronic devices such as GaAs MESFET, the InP MISFET and the HEMT have also been demonstrated. Thus, electronic and optical devices may potentially be integrated monolithically on the same chip. The advantages of integrated opto-electronic signal processing include high speed of operation (due to short interconnection delay time), versatility in combined optical-electronic signal processing schemes and reliability and convenience of optical-electronic signal conversion. However, the conventional electro-optical coefficients in III-V semiconductors are an order of magnitude smaller than that of $LiNbO_3$ which is already an order of magnitude or more smaller than that of liquid crystals or PLZT ceramics. In order to realize effectively the combined opto-electronic signal processing, we need either (a) to find a new interaction mechanism in III-V semiconductors that will produce a large electro-optical effect or strong optical interactions, or (b) to concieve combinations of devices such as lasers, detectors and

transistors that are interconnected in a pixel in such a manner that will perform the signal processing function from the photo-excited carriers without using either the electro-optical or the nonlinear optical coefficient. Thus, during FY 1984 and part of FY 1983 we have undertaken (a) a study of the electro-refraction effect, (b) a study of the cross modulation effect of optical radiations at two wavelengths, and (c) a study of interconnected devices that will perform logic functions electrically from the photo excited carriers of optical radiations at two different wavelengths. These studies have not been completed. They have been transferred into a new AFOSR Grant (No. 84-0389) with UCSD. In section 3 of this final report we will present the data that have been obtained under AFOSR Grant 80-0037.

2. Research on Chirped Grating Lenses

Currently the most commonly used guided-wave lens is a geodesic lens that requires individual precision grinding of the non-spherical surface contour for each lens [1,2]. Such a fabrication process is expensive, and the geodesic lens is difficult to integrate with other devices. Lens effects can also be obtained by diffraction from chirped grating surface relief patterns illustrated in Figure 1. Such surface relief patterns can be made by the much less expensive planar micro-fabrication techniques. We have investigated earlier the Fresnel lenses. They have given diffraction limited spot size and large angular field of view[3-5]. But their efficiency was less than 50%. Chirped grating lenses are similar to the Fresnel lenses, except the grating grooves are long, and volume interaction is used to obtain high efficiency. From another point of view, both the chirped grating lens and the Fresnel lens can be regarded as a one

dimensional hologram, one is thin phase hologram and the other one is a thick volume hologram. However, they differ from the conventional holograms in that a much more sophisticated pattern of the index variation can be designed by computer analysis and fabricated by photo lithography and planar microfabrication processes. For example, Figure 2 shows a curved chirped lens where the grooves are curved to satisfy more accurately the phase matching condition when the F-number is small or when the grooves need to be long. Chirped grating lenses with efficiencies as high as 90% have been reported[6-9]. However, the combination of high efficiency η and large angular field of view $\Delta\theta$, or the combination of high efficiency η and small F-number requires special design optimization and materials and fabrication control. In this grant, the first task that we have accomplished was the formalism of a generalized coupled mode theory, published in IEEE Trans. MTT, MTT-29, 881 (1981) [10]. We used that as a design tool to calculate the effect on the phase and the amplitude of the diffracted beam when the grating periodicity, groove length, groove shape, material indicies, incident beam angle, incident beam profile and fabrication tolerances are varied. However, the generalized coupled mode analysis is inaccurate whenever there is significant power in higher order diffracted beams. Thus we have formulated a perturbation and iterative analysis for lenses with medium Q factor values. This was published in the IEEE Journal of Quantum Electronics QE-20, 410 (1984)[11]. We have also performed experimental studies of the higher orders of diffraction and showed that the rigorous coupled wave analysis by M. G. Moharam and T. K. Gaylord[12] could predict accurately the power diffracted into the higher orders, thereby providing a quantitative assessment of the errors of using our generalized coupled mode analysis for the design of chirped grating

lenses. This work has been published in Applied Optics on January 15th, 1985[13]. The second task that we have accomplished is to investigate experimentally and theoretically the performance and the limitations of chirped grating lenses on Ti-indiffused $LiNbO_3$ waveguides. The lens on this waveguide is important to the integrated optical r.f. spectrum analysis of radar signals. This work also provided the basis for the comparison of the lens properties that might be obtained by various approaches for the joint TRW-UCSD program. Here, we have developed experimental processes to fabricate various grating lenses including the deposition of rutile grooves and the use of the reactive ion beam technique to etch the grooves on such waveguides. High efficiency, over 80%, was obtained routinely. However, the combination of large angular field of view (e.g. larger than 2 degrees) and high efficiency or the combination of small F-number and high efficiency is difficult to obtain because of the material properties of Ti-indiffused waveguides. For chirped grating lenses large index perturbation (i.e. large coupling coefficient between the incident and the diffracted beams) is necessary for obtaining high efficiency at small groove lengths (e.g. 25 to 50 μm). Small groove lengths are also needed for small F-numbers or large angular field of view. In the Ti-indiffused waveguide the material index of the waveguiding layer is very close to the material index of the substrate. Large index perturbation by using either a high rutile groove profile or deep etched grooves will cause either substantial amounts of substrate mode conversion or a second propagating mode. Thus the angular field of view or the F-numbers are limited by the material properties of the Ti-indiffused waveguide. The results of this study were published in the Journal of Lightwave Technology, LT-2, 503 (1984)[14]. Two alternate methods were also conceived and demonstrated that would circumvent this

difficulty. One is to use ion exchanged waveguides (published in Applied Physics Letters 43, 424 (1983), the second one is to use a Nb_2O_5 transition waveguide for the lens section (published in Applied Optics, 22, 3128 (1983) [9,10]. A moderate improvement of the magnitude of index perturbation can also be obtained by controlling the Ti-indiffusion process as reported in Applied Physics Letters, 45, 207 (1984) [15]. The third task we have accomplished is to investigate the fundamental limitations of the performance of chirped grating lenses in all waveguides caused by the index perturbation that can be realized in existing materials, (to be published January 1985, in the Journal of Quantum Electronics), the resolution of the lithographic process, diffraction into higher orders (to be published January 1985 in Applied Optics) and the tolerance of the microfabrication processes (to be published January 1985 in Applied Optics [13,16,17].

A scientific report summarizing the properties of chirped grating lenses in optical waveguides was prepared and issued under this grant on October 1st, 1984.

3. Research on Electro-Optical Properties of III-V Semiconductors

There are two objectives in our program: (a) To find an interaction mechanism in III-V semiconductors that will produce a large electro-optical effect or strong optical interactions. (b) To conceive combinations of devices such as lasers, detectors and transistors that are interconnected in a pixel in such a manner that will generate electronically the signal processing function from the carriers photo-excited by the optical radiations, without using the electro-optical coefficient. Ultimately nonlinear optical interactions may be utilized to achieve modulation at frequencies much beyond the microwave range.

So far, we have undertaken three research tasks. (a) A study of the electrorefraction effect near the bandgap of the III-V semiconductors (GaAs and InP). The change of refractive index due to an applied electric field is expected to be very large for wavelengths near the bandgap. A combination of electroabsorption and electrorefraction may be utilized to provide effective electro-optical modulation. (b) A study of the cross modulation of the radiation at wavelength λ_1, near the bandgap by a second radiation above the bandgap at wavelength λ_2. Cross modulation may be utilized to obtain an AND logic function between these two radiations. (c) A study of the characteristics of a photo-conductive detector in InP coupled with a photo-diode in InGaAs. Both devices are integrated on the same chip which consists of a layer of GaInAs grown epitaxially on InP. The objective of this study is to demonstrate the AND logic function of two radiations at λ_R ($\simeq$ 0.84 μm) InP and λ_ℓ ($\simeq$ 1.5 μm). The logic function is realized electrically by means of the carriers photo-excited in InP by λ_s and in GaInAs by λ_ℓ. The technical details of these three research tasks undertaken in this AFOSR grant are summarized in the following subsections, 3.1, 3.2 and 3.3.

These studies have not been completed, they are being continued under the new AFOSR grant (84-0389).

3.1 Electrorefraction and Electroabsorption in InP and GaAs Near the Bandgap

The immediate objective of this work is to measure the electrorefraction and electro-absorption in bulk III-V semiconductors, i.e. to determine the changes in the refractive index n and absorption coefficient α respectively caused by an applied electric field at various optical wavelengths near the fundamental absorption edge. This data is required

later for the design of electro-optic modulators and optical digital and analog data processing elements.

So far, measurements of changes in index and in absorption have been made on two bulk materials, InP and GaAs, since these materials are readily available commercially. In order to apply large voltages to the samples without heating them significantly, high resistivity material is required. Such high resistivity is avialable from semi-insulating materials which we have used exclusively. Our experiment involves propagating an optical beam through a thin sample and applying an electric field in the same direction as the optical beam. This required the following sample preparation: A piece of a wafer was optically polished on both sides. Indium tin oxide, a transparent conductor, was deposited on both polished surfaces. On top of that a layer of aluminum was deposited, with a window opened in the aluminum so that light can propagate through the sample. The purpose of the aluminum layer is to reduce the resistivity of the electrode.

In order to evaluate electrorefraction and electroabsorption as a function of wavelength a tunable pulsed infrared laser source is used. Our source is a Chromatix CMX-4/IR optical parametric oscillator driven by a Chromatix CMX-4 dye laser. In order to determine a small change of refractive index, we have chosen to measure the refractive index interferometrically. We have used a Mach-Zehnder interferometer becuase it is least sensitive to absorption in the sample. The interferometer is illustrated schematically in Figure 3. The sample is placed in one arm of the interferometer. In the other arm is an optical wedge mounted on a micrometer-drive translation stage, which is used to precisely control the phase of the reference beam. An attenuator may also be placed in this arm. Interference fringes are visible at the output of the interferometer. As an

electric field is applied to the sample the refractive index changes, causing the fringe position to shift. The fringe shift is measured and from it the change of refractive index is calculated. In the electro-absorption measurements, transmission through the sample was measured.

Initially a Vidicon camera was used to observe the fringe pattern, and measurements of the fringe shift were made by counting complete or fractional "steps" of the fringes. This technique produced some results, but it was not satisfactory for two reasons. First, for refractive index changes of the magnitude observed this technique is not sensitive enough to give accurate results. Second, this technique provides no information about the speed of the refractive index change, since the response time of the Vidicon is about one second.

We have now implemented an improved interferometer monitoring system with sensitivity better than one hundredth of a fringe. The system utilizes an electronically sampled silicon photodetector coupled with a computer to measure accurately the fringe pattern of the interferometer with and without the applied voltage. In principle, a single photodetector could be used, although we have used a bicell (two photodetectors side by side on a single chip) for better sensitivity. The bicell measures the spatial derivative of the intensity at any point of the interference fringe pattern. For a given position of the optical wedge (i.e. the phase of the reference beam) the output of the bicell in response to each laser pulse is amplified and sampled by a 12 bit analog to digital converter interfaced with a computer. Hundreds of data samples are averaged by the computer, giving a very accurate measurement of the intensity for a given phase of the reference beam, in spite of vibrations in the fringe pattern. An entire cycle of the interference fringe pattern is obtained by translating

the optical wedge to scan the phase of the reference beam. Thus the sinusoidal interference fringe pattern is recorded with and without the applied voltage, and the difference in phase is computed by comparing positions of zero-crossings in the two fringe patterns. The speed of this measurement system is limited only by the pulse generator, not by the detector. The resolution of this system is about 10 milliradians of phase degrading by a factor of 3 or 4 at short wavelengths where very little light is transmitted through the sample.

The experimentally measured results of electroabsorption in InP and GaAs are shown in Figure 4. For comparison, previously published results[18] are shown as crosses in the same graph. The experimentally measured electro refraction data are shown in Figures 5 and 6 for InP and GaAs respectively. Note that large change in index Δn is obtained only when the optical wavelength is close to the bandgap where there is strong electroabsorption. For the protection of our samples, voltages have been limited to 150 V across the .10 mm thick InP sample, and 250 V across the .45 mm thick GaAs sample.

We have investigated the effect of laser intensity on electroabsorption. For InP, laser intensities up to 0.3 W/cm^2 have no effect on the measured electroabsorption. With higher intensity electroabsorption increases slightly. Similar results were obtained for GaAs; both electroabsorption and electrorefraction are constant up to 0.1 W/cm^2 and increase slightly at higher intensities. The InP measurements reported here were all made at low intensity. For the GaAs measurements the optical intensity was not monitored; this may introduce an error of up to 30%.

In our very first electrorefraction measurement we observed a very large index change (Δn = .006) which occurred only after the sample had

12. Christopher Warren, Siamak Forouhar and William S. C. Chang, "Double Ion Exchanged Chirped Grating Lens in Lithium Niobate Waveguides", Appl. Phys. Lett., 43, 424-426 (1983).

13. Siamak Forouhar, Ron-Xin Lu, William S. C. Chang, Richard L. Davis and Shih-Kay Yao, "Chirped Grating Lenses on Nb_2O_5 Transition Waveguides", Appl. Optics, 22, 3128-3132 (1983).

14. S. Forouhar, W. S. C. Chang and S. K. Yao, "Chirped Grating Lenses in Ti-Indiffused $LiNbO_3$ Planar Waveguides", 4th International I.A.O.C. Conference, Tokyo, Japan, June 27-30th, 1983.

15. T. Findakly and S. K. Yao, "Chirped Grating Lenses on $LiNbO_3$ by Benzoic Acid Treatment", Fourth International Conference on Integrated Optics and Optical Fiber Communications, Tokyo, Japan, June 27th-30th, 1983.

16. S. Forouhar and W. S. C. Chang, "A Perturbation and Iterative Perturbation Analysis of Linearly Chirped Grating Lenses of Medium Q in Dielectric Waveguides", IEEE J. of Quantum Electronics, QE-20 No. 4, 410-417 (1984).

17. S. Forouhar, W. S. C. Chang and S. K. Yao, "Performance and Limitations of Chirped Grating Lenses on Ti-indifussed $LiNbO_3$ Planar Waveguides", Journal of Lightwave Technology, LT-2, No.4, 503 (1984).

18. J.-M. Delavaux and W. S. C. Chang, "Design and Fabrication of Efficient Diffraction Transmission Gratings on Step Index Optical Waveguides", Applied Optics, 23 ,No. 17, 3004 (1984).

7. W. S. C. Chang, S.-T. Zhou, Z.-Q. Lin, S. Forouhar and J. M. Delavaux, "Performance of Diffraction Lenses in Planar Optical Waveguides", The Third International Conference on Integrated Optics and Fiber Optics Communications, San Francisco, 1981 (April).

8. W. S. C. Chang, "The Effects of Materials Technology and Fabrication Tolerances on Guided-Wave Optical Communication and Signal Processing", a Chapter of the book: VLSI Electronics Microstructure Science, Vol. 3, Norman Einspruch (Editor), Academic Press (1981).

9. J.-M. Delavaux, S. Forouhar, W. S. C. Chang and R.-X. Lu, "Experimental Fabrication and Evaluation of Diffraction Lenses in Planar Optical Waveguides", paper presented to IEEE/OSA CLEO '82, April 14-16, 1982, Phoenix, Arizona.

10. W. S. C. Chang, S. Forouhar, J.-M. Delavaux and R.-X. Lu, "Fabrication and Performance of Diffraction Lenses", SPIE Technical Symposium, Los Angeles, 1982 (January).

11. William S. C. Chang, S. Forouhar, J. M. Delavaux, C. Warren and R.-X. Lu, "Chirped Grating Lenses in Ti-Indiffused $LiNbO_3$ Optical Waveguides", paper presented at the European Conference on Optical Systems and Applications, 7th-10th September, 1982, Edinburgh, Scotland. Published in the Proceedings of the ECOSA '82, SPIE Vol. 369, pp.581-590, 1982.

5. Papers Presented, Published and Submitted

1. W. S. C. Chang and P. R. Ashley, "Fresnel Lenses in Optical Waveguides, IEEE Journal of Quantum Electronics, QE-16, 744 (1980).

2. Z.-Q. Lin, S.-T. Zhou, W. S. C. Chang, S. Forouhar and J. Delavaux, "A Generalized Two-Dimensional Coupled Mode Analysis of Curved and Chirped Periodic Structures in Open Dielectric Waveguides", MTT Transactions, MTT-29, 881 (1981).

3. W. S. C. Chang, Z.-Q. Lin, S.-T. Zhou, J. Delavaux and S. Forouhar, "The Fresnel and Chirped Grating Lenses in Optical Waveguides", Proceedings of SPIE Technical Symposium, Vol. 269, p.105, North Hollywood, 1981 (February).

4. S. Forouhar and W. S. C. Chang, "Analysis of Chirped Grating Lenses", 1980 IEEE MTT-S International Microwave Symposium, May 28th-30th 1980, Washington D. C.

5. W. S. C. Chang, Z.-Q. Lin, S.-T. Zhou, J. Delavaux and S. Forouhar, "The Fresnel and Chirped Grating Lenses in Optical Waveguides", SPIE Technical Symposium, Los Angeles 1981 (February).

6. Z.-Q. Lin, S.-T. Zhou, W. S. C. Chang, S. Forouhar and J. Delavaux, "A Generalized Two-Dimensional Coupled Mode Analysis of Curved and Chirped Periodic Structures in Open Dielectric Waveguides", MTT International Symposium, Los Angeles, 1981 (June).

4. Conclusion

In conclusion, we have made a substantial contribution in the guided wave chirped grating lens technology. Our work indicates that high efficiency and diffraction limited spot size can always be obtained. However, one must combine materials technology with theoretical design in order to realize combinations of high efficiency and large angular field of view or high efficiency and small F-number. For example, an angular field of view of several degrees and efficiency larger than 80% can be obtained in $LiNbO_3$. Since FY 1983 we have initiated a new area of study on the electo-optical material and device properties of III-V semiconductors. The research program is important for optical signal processing and fiber communications applications. More specifically we have found very large electro-optical changes in the index occuring at a wavelength near the bandgap of GaAs and InP. Effective modulators may be designed in the future using this effect. We have discovered a cross modulation effect in SI GaAs produced by a laser radiation above the bandgap on a LED radiation near the bandgap. Such a cross modulation effect may be utilized in the future to achieve an "AND" gate logic function. We have begun the investigation of a photoconductive detector at λ = 0.84 μm coupled in series with a photodiode at λ = 1.5 μm. Such a coupled device may again serve the purpose of an "AND" gate logic function. Work in the electro-optical properties of III-V semiconductor will continue in a new AFOSR grant, No. 84-0389.

the slope of the $1/R_s$ vs. P curve is decreased slightly at P > 4 mw because of a slight decrease in mobility and in lifetime when there is a large number of photoexcited carriers. For P < 4 mw the slope of $1/R_s$ vs. P is 2.5×10^{-2} $w^{-1}ohm^{-1}$. If we use a simple model of an InP sample with width w, thickness D and length L, the resistance will be given by

$$\frac{1}{R_s} = \frac{q(\mu_n + \mu_p)\tau\eta}{h\nu L^2} P$$

Here we have L = 50 μm, hν = 1.48 eV and $\mu_n + \mu_p = 0.48$ $M^2/V\text{-}S$. Y. Hori et al. gave the lifetime τ as 350 p.sec[25]. Thus, we obtain η = 0.57 for our photoconductive detector. These photoconductive detectors also exhibit breakdown like I-V behavior in the dark. The breakdown voltage is 75 V at 10 μm gap of separation between the electrodes, or 120 V at 20 μm gap.

Due to the breakdown of our Nd/YAG pumped color center laser, we were not able to evaluate the GaInAs/InP diode at 1.5 μm wavelength. We have used a focused beam of 0.84 μm wavelength laser to illuminate the photoconductive detector and then measured the I-V curve of the back biased GaInAs/InP photodetector in series with the illuminated InP photoconductive detector and a forward biased GaInAs/InP photodetector. Figure 21 shows the measured I-V characteristics. Notice that when $V > V_B$, the current is still limited by the resistance of the photoconductive detector. So the slope of the I-V curve for $V > V_B$ is dependent on the power P as shown in Figure 22.

characteristics of a photo-conductive detector in response to the radiation at λ_s = 0.84 μm wavelength is expected to behave like that shown in Figure 17b. Thus, the I-V characteristics of the two devices in series is expected to behave like that shown in Figure 17c. If the radiations at λ_s and λ_ℓ are illuminating the device from the back side as shown in Figure 15a, and if the InP substrate is thicker than the absorption length then the radiation at 0.84 μm will only be detected in the photoconductive detector region. Hence, at the bias voltage of V_o, the devcie will function as an AND gate for the two radiations at λ_s and λ_ℓ.

P-$In_{0.53}Ga_{0.47}As$/SI-InP samples were grown by LPE at the Naval Ocean Systems Center (NOSC), San Diego. The material properties are listed in Table I and Table II. From the data shown in these two tables, the energy-band diagram has the form sketched in Figure 18. In the initial devices and for the sake of simplicity, we did not etch any windows in the back side as shown in Figure 15. Focused radiation is used to illuminate the sample from the front side. The device pattern on the front side is obtained by ion milling under a mixture of 80% Ar/20% O_2 fro 35 minutes, followed by Reactive Ion Beam Etching (RIBE) under C_2F_6 for 15 minutes then followed by chemical etching in $HCl/CH_3COOH/H_2O_2$ for 10 to 20 seconds to remove the damage created by the ion beams. Photo-resist (post baked at 140°C for 2 hours) is used as the mask. Figure 19 is a micro-photograph of a processed device.

In order to investigate photoconductive detection in InP, we have made a pair of Au-Ge (88%/12%) electrodes on SI InP by the lift-off photolithography process. For an InP photoconductor, we expect its resistance to be inversely proportional to the power P illuminating the detector. Figure 20 shows the experimental $1/R_s$ vs. P curve that we have obtained. We think

3.3 The Study of a Coupled Photodiode and Photoconductive Detector

Recently many InGaAs optical devices such as lasers and detectors have been investigated. They are particularly suited for fiber communication applications because they could function in the 1.5 μm wavelength range. InGaAs and InP also have very high saturation electron mobility. InP and InGaAs transistors are also of interest for high speed electronic applications provided some of the material problems can be resolved in the future. $In_{0.53}Ga_{0.47}As$ is also lattice matched to InP. $In_{0.53}Ga_{0.47}As$ can be grown epitaxially on InP substrates by LPE or by MBE methods. Potentially, optical and electronic devices can be monolithically integrated on InGaAs/InP or InGaAsP/InP. Thus we have been examining various potential interconnected opto-electronic devices based on the InGaAs/InP material structure that can provide signal processing functions such as an AND gate. The structure of the specific device that we have been investigating in FY 1984 is shown in Figure 15 with its equivalent electrical circuit shown in Figure 16. It consists of essentially a forward biased p-InGaAs/SI InP photodiode, a SI InP photoconductive detector and a p-InGaAs/SI InP reverse biased photodiode in series. The forward biased photo-diode acts simply as a short circuit. Thus the interconnected device functions essentially as a photoconductive detector in series with a reverse biased photodiode. If a resistor R_0 is connected in series with that, we can describe the characteristics of such a device by the equivalent circuit shown in Figure 16. Let us set aside for the time being the various material problems that might be associated with a GaInAs/InP diode and consider just an ideal photo-diode. The I-V characteristics of a reverse biased photodiode in response to the radiation at λ_ℓ = 1.5 μm or shorter is expected to behave like that shown in Figure 17a, while the I-V

probably caused by the RC time constant of the electrical circuit. (2) In the second experiment we monitored the voltage across the sample when λ_2 radiation pulse is applied. We see clearly there is a drop in this voltage during the λ_2 pulse. Thus, it appears that the cross modulation effect observed during the λ_2 pulse could be explained by the fact that the drop in voltage induced by the photoexcited carriers will lead to a drop in the electric field across the sample, resulting in a drop in the electroabsorption effect. In the third experiment we varied λ_2. (3) Figure 14 shows the photo current, the attenuation of the LED light at λ_1 and the reduction in the voltage across the GaAs sample during the λ_2 radiation pulse as a function of the λ_2 wavelength. Clearly the cross modulation effect is a maximum when λ_2 is at the band edge. We attributed the drop in cross modulation at wavelength shorter than the bandgap to the drop in photo current at the shorter wavelength. However, it is not yet clear why the photocurrent should be reduced rapidly at the wavelength shorter than the absorption edge. We have also not been able to determine the mechanism through which the attenuation at λ_1 is increased after the radiation pulse at λ_2.

In conclusion, we have demonstrated a new cross modulation effect in SI GaAs. A number of the side effects have not yet been explained. The situation is also complicated because the carrier relationship in SI GaAs is very complex and difficult to understand. We plan to conduct the same experiment in other materials usch as SI InP or other heterostructures in the future so that we can understand this cross modulation effect better. We will also assess the practical device performance characteristics that may be obtained from such a cross modulation effect.

affected by the first pulse when the separation is more than 25 μsec. (b) In Figure 10 the attenuation at λ_1 is increased after the λ_2 pulse. We have measured the change in attenuation at λ_1 due to the applied electric field after the occurance of the optical radiation pulse at λ_2. We found that the change in attenuation at λ_1 is increased substantially after the λ_2 pulse, beyond what was possible without radiation pulse at λ_2. If a second voltage pulse is applied, the attenuation at λ_1 during the second voltage pulse will also be increased with the presence of the λ_2 radiation pulse during the first voltage pulse, when the separation of two voltage pulses is less than 5 microseconds. (c) Moreover, the increase in attenuation at λ_1 after the λ_2 pulse has a nonlinear dependence on the intensity of the λ_2 radiation. Figure 12 shows the attenuation at λ_1 as a function of the applied voltage when the intensity of the λ_2 radiation is 0.059×10^{-3} joules/second and 0.085×10^{-5} joules/second. Thus it appears that the carriers generated by the λ_2 pulse have created additional absorption at λ_1 within a relaxation time of the order of 10 microseconds. Additional experiments have been performed in order to understand some of these side effects. (1) In the first experiment we changed the RC time constant of the electrical circuit connected to the voltage pulse generator by introducing a 5×10^{-3} μ-farad capacitor across the voltage source. The measured transmitted LED light as a function of time without this additional capacitor is shown in Figure 13a and the transmitted LED light with the additional capacitor is shown in Figure 13b, without any radiation at λ_2. Clearly the electroabsorption in the second pulse is larger with the capacitor. We think the increase in attenuation at λ_1 as a function of time both within the first voltage pulse and in the second voltage pulse following immediately the first voltage pulse is

LED light is increased due to the electroabsorption effect as shown in Figure 9. The measured increase in attenuation is 4 to 5% at 300 volts, it agrees only roughly with other available published electroabsorption data[18], because the LED has an extended spectral width and because the absorption edge of SI GaAs is not very abrupt. The electroabsorption is also in rough agreement with our own electroabsorption data shown in Figure 4. When the sample is illuminated within the voltage pulse duration by the pulsed radiation at λ_2 at an intensity of 600 watts/cm^2, the increase in attenuation due to electroabsorption is reduced to zero as shown in Figure 10 when λ_2 is present. In other words, under a large applied electric field, the LED light is transmitted to the detector with no electroabsorption, only when both the radiation at λ_1 and λ_2 are present. Thus we have demonstrated a cross modulation effect. This effect performs essentially the logic function of an optical "AND" of the radiations at λ_1 and at λ_2.

A number of side effects have also been observed. (a) We have measured the change of attenuation at λ_1 without the pulsed radiation at λ_2, as a function of the applied voltage and at a variable time delay from the leading edge of the voltage pulse. It is interesting to note that the change in attuation increases as the delay time is lengthened and saturates after approximately 25 microseconds of delay. Figure 11 shows the increase in attenuation as a function of applied voltage at zero time delay and at 25 μsec. time delay. When we measured the increase in attenuation produced by two consecutive pulses, we observed that the change in attenuation during the second pulse is affected significantly by the first pulse when the two pulses are close to each other (less than 5 μsec. delay between pulses), and the attenuation characteristics during the second pulse is not

another Al layer on top of the InSnO layer, leaving just a small window for the light to pass through the transparent InSnO electrode. The basic experimental setup is illustrated in Figure 7. A beam of light from a LED source (10 mwatts) centered at λ_1 = 0.88 μm is transmitted through the window in the sample. The LED light source has an aperture lens and a half angle spread of 6°. After transmission through the GaAs, the LED light is focused on to a photo detector. Some part of the LED spectrum fell below the absorption edge (see Figure 8). A second radiation at the wavelength λ_2 = 0.8850 ± 0.01 μm, obtained from the tunable chromatix CMX-4/IR optical parametric oscillator which is driven by a chromatix CMX-4 dye laser, is also available to transmit at an angle of incidence of 30° to the substrate normally through the same window region as the LED light. This radiation source has a maximum intensity of 1 kwatt/cm^2 and microsecond of pulse duration, with λ_2 tunable from the visible light wavelength to 2 μm in the infra-red. The optical energy per pulse can be adjusted from 10^{-8} jouls to 10^{-4} jouls with a pulse to pulse energy fluctuation of 20 to 30%. In addition, a voltage pulse generator with variable pulse width (few tens of microseconds) and height (maximum 1000 volts) is used to provide the applied voltage to the GaAs sample. The pulse radiation at λ_2 can be triggered in synchronization with the voltage pulse so that the optical pulse can be controlled to occur at certain specific positions in time during the voltage pulse. Triggering for the voltage pulse generator has also been provided so that two consecutive voltage pulses can be applied to the sample with a variable time delay between the two voltage pulses.

When a voltage pulse of few tens of microseconds duration at 300 volts (corresponding to an electric field of 7.5 KV/cm) is applied to the InSnO/Al electrodes in the absence of λ_2 radiation, the attenuation of the

This work has been submitted for presentation in the 1985 CLEO meeting.

3.2 Cross Modulation of Light in Semiconductor Materials in the Presence of Electric Fields

A variety of optical devices are now being investigated for optical signal processing and communication[22,23]. Various forms of bulk semiconductor bistable devices have been reported[22]. Recently, multiple-quantum-well (MQW) structures have shown good potentials for signal processing and communication applications[23,24]. We have observed cross modulation of radiation at wavelength λ_1, (below and near the bandgap) induced by a second radiation at wavelength λ_2, (above the bandgap) in bulk GaAs in the presence of an applied electric field. This effect could potentially be used to obtain optical logic functions such as the AND gate. Such effects are expected to exist in other direct bandgap III-V compound semiconductors such as InP and to be much larger in MQW structures. In the following we will present the data that we have obtained in GaAs in FY 1984.

In the initial experiments, we have used an undoped Semi-Insulating (SI) GaAs sample. Both sides of the sample are optically polished. The carrier density was given by the manufacturer as 10^8 per cm^3. The samples are approximately 400 μm thick. A layer of transparent InSnO electrode approximately 600 A thick was sputtered on to the two polished GaAs surfaces to form a transparent electrode. Since the resistance of such an InSnO electrode was fairly high (the sheet resistance was approximately 1,000 to 10,000 ohms/□) and since the high resistance may cause distortion of the electric voltage pulses appearing across the GaAs, we evaporated

measured electroabsorption is much larger than the predicted value. This may be caused by those effects mentioned above which are not included in the simple theory.

Electroabsorption is a fundamental physical phenomenon, and electrorefraction is derived from it by the Kramers-Kronig relationship[21]. It may seem inconsistent that the measured electrorefraction fits the theory while the electroabsorption from which it is derived does not. However, we have measured the electroabsorption over only a small portion of the wavelength spectrum. One would expect the electrorefraction to be affected more by the large electroabsorption, on the order of 10^3 cm^{-1} to 10^4 cm^{-1}, occurring closer to the absorption edge, than by the small electroabsorption that we have observed .015 μm to .040 μm away from the absorption edge. It appears that the simple theory can account for the observed electrorefraction even though it can not account for the observed electroabsorption.

A useful figure of merit for an electro-optic material is the ratio $\Delta n/E$, the change of refractive index divided by the applied electric field. For the Pockels effect, this ratio has the value $\Delta n/E = \frac{1}{2} n^3 r_{41} = 26 \times 10^{-12}$ m/V for both InP and GaAs and for $LiNbO_3$, $\Delta n/E = \frac{1}{2} n_e^3 r_{33} = 160 \times 10^{-12}$ m/V. In our experiments the maximum $\Delta n/E$ measured was 240×10^{-12} m/V for InP and 190×10^{-12} m/V for GaAs. Thus, this type of electrorefraction effect can provide electro-optic modulation in InP and GaAs greater than the Pockels effect in $LiNbO_3$ and nearly an order of magnitude greater than the Pockels effect in InP and GaAs. In addition, III-V semiconductors offer the possibility of integrating electro-optic modulators on the same chip with other electronic and optoelectronic devices.

suffered some kind of electrical breakdown. This index change had a time constant of several seconds. We do not yet know for certain the cause of this slow index change. In the measurements reported here we want to be certain that the changes Δn and $\Delta\alpha$ that we measure are fast, not slow, effects. Therefore, we have investigated the effect of the duration of the electrical pulse on the electroabsorption. An electrical pulse 5 msec in length is applied to the sample, and within the duration of the electrical pulse the instant at which the short laser pulse is applied is varied. For InP we found that there is no change in the electroabsorption when the instant of the laser pulse is varied form the time the electrical pulse reaches its full height until 5 msec later. The observed speed of response of the electroabsorption in this measurement was limited by the rise time, 20 μsec, of the electrical pulse generator; the effect is probably much faster than 20 μsec. For GaAs, however, it appears that after the electrical pulse reaches its full height the electroabsorption continues to rise, saturating after about 100 μsec to a value roughly 25% higher than the initial value. The GaAs results reported here were taken with an electrical pulse long enough for the electroabsorption to saturate.

A simple theory for computing electroabsorption and electrorefraction has been described in the literature[19,20]. This simple theory neglects several important effects such as thermal broadening, impurity absorption, free carrier absorption and excitonic absorption. Nevertheless, the curves in Figures 4, 5 and 6 represent the calculated electroabsorption and electrorefraction based upon this theory. For electrorefraction in InP, there is good agreement between experiment and theory. For GaAs the experimental data are qualitatively similar to, but quantitatively several times larger than, the theoretical prediction. For both InP and GaAs the

19. J.-M. Delavaux and W. S. C. Chang, "Fundamental Limitations in the Performance of Chirped Grating Lenses on Planar Optical Waveguides", J. Quantum Electronics, (to be published January 1985).

20. J.-M. Delavaux, W. S. C. Chang and M. G. Moharam, "Comparison of the Experimental and Theoretical Diffraction Characteristics of Transmission Gratings on Planar Dielectric Waveguides," Applied Optics, (to be published 1985).

21. J.-M. Delavaux and W. S. C. Chang, "Investigation of the Effect of Fabrication Tolerances on the Diffraction Performance of Chirped Grating Lens on Planar Optical Waveguides," Applied Optics (to be published 1985).

22. S. Forouhar, G. E. Betts and W. S. C. Chang, "Effects of Water Vapor on Modes in Ti-Indiffused $LiNbO_3$ Planar Waveguides", Appl. Phys. Lett., 45, 207 (1984).

23. B. Zhang, S. Forouhar, S. Y. Huang and W. S. C. Chang, "C_2F_6 Reactive Ion Beam Etching of $LiNbO_3$ and Nb_2O_5 and Their Application to Optical Waveguides", J. of Lightwave Technology, LT-2, No.4, 528 (1984).

24. B. Zhang, J.-M. Delavaux and W. S. C. Chang, "Ion Beam Etching of BaO and Glass and SiO_2 Thin Films and Their Application to Optical Waveguides", Appl. Optics, 23, 773 (1984).

25. T. E. Van Eck, L. M. Walpita, W. S. C. Chang and H. H. Wieder, "Electro-refraction and Electroabsorption in InP and GaAs Near the Bandgap", paper submitted for presentation to the 1985 CLEO Conference.

26. L. M. Walpita, W. S. C. Chang, H. H. Wieder and T. Van Eck, "Cross Modulation of Light in Semiconductor Matierals in the Presence of Electric Fields", paper submitted for presentation in the 1985 Topical Meeting on Picosecond Electronics and Opto-Electronics.

27. J. M. Delavaux and W. S. Chang, "Fundamental Diffraction Limits of the Performance of Chirped Grating Lenses", IEEE/OSA, Topical Meeting of Integrated and Guided Wave Optics, Orlando, Florida, April 23-26, 1984.

28. S. Forouhar, G. E. Betts and W. S. C. Chang, "Effects of Water Vapor on Modes in Ti-indiffused $LiNbO_3$ Planar Waveguides", Annual Meeting of the American Ceramic Society, Pittsburgh, April 1984.

29. J.-M. Delavaux, G. E. Betts and W. S. C. Chang, "Electro-Optic Linear Chirped Grating Lenses on Planar Optical Ti:$LiNbO_3$ Waveguides", to be published in J. Lightwave Technology, 1985.

30. J-M. P. Delavaux, G. E. Betts and W. S. C. Chang, "Electro-Optic Chirped Grating Lenses on Planar Optical Ti:$LiNbO_3$ Waveguides", paper presented in the 1984 Annual Meeting of the Optical Society of America, October 1984.

6. References

1. C. M. Verber, D. W. Vohey and V. W. Wood, Appl. Phys. Lett. 28, 514 (1976).

2. G. E. Betts and G. E. Marx, Appl. Optics, 17, 3969 (1978).

3. W. S. C. Chang and P. R. Ashley, J. Quantum Electronics, QE-16, 744 (1980).

4. S. Valette, A. Morque and P. Motier, Elect. Lett. 18, 13 (1982).

5. T. Suhara, K. Kobayashi, H. Nishihara and J. Koyama, Appl. Optics, 21, 1966 (1982).

6. S. K. Yao and D. E. Thompson, Appl. Phys. Lett. 33, 635 (1978).

7. S. Forouhar and W. S. C. Chang, "Fabrication and Evaluation of Chirped Grating Lenses in Lithium Niobate Waveguides", Technical Report, University of California, San Diego (1983).

8. S. Forouhar, R. X. Lu, W. S. C. Chang, R. L. Davis and S. K. Yao, Appl. Optics 22, 3128 (1983).

9. C. Warren, S. Forouhar, W. S. C. Chang and S. K. Yao, Appl. Phys. Lett., 43, 424 (1983).

10. Z. Q. Lin, S. T. Zhou, W. S. C. Chang, S. Forouhar and J. M. Delavaux, IEEE Trans. MTT, MIT-29, 881 (1981).

11. S. Forouhar and W. S. C. Chang, IEEE J. Quantum Electronics, QE-20, 410 (1984).

12. M. G. Moharam and T. K. Gaylord, J. Opt. Soc. America, 71, 811 (1981).

13. J. M. P. Delavaux, W. S. C. Chang and M. G. Moharam, "Comparison of the Experimental and Theoretical Diffraction Characteristics of Transmission Gratings on Planar Dielectric Waveguides", to be published in Applied Optics.

14. S. Forouhar, W. S. C. Chang and S. K. Yao, J. of Lightwave Tech., LT-2, 503 (1984).

15. S. Forouhar, G. E. Betts and W. S. C. Chang, Appl. Phys. Lett., 45, 207 (1984).

16. J. M. P. Delavaux and W. S. C. Chang, "Fundamental Limitations in the Performance of Chirped Grating Lenses on Planar Optical Waveguides", to be published in J. of Quantum Electronics, January 1985.

17. J. M. P. Delavaux and W. S. C. Chang, "Investigation of the Effect of Fabrication Tolerances on the Diffraction Performance of Chirped Grating Lens on Planar Optical Waveguides", to be published in Appl. Optics.

18. G. E. Stillman, C. M. Wolfe, C. O. Bozler and J. A. Rossi, Appl. Phys. Lett. 28, 544 (1976).

19. D. E. Aspnes and N. Bottka in Semiconductors and Semimetals, Vol.9, edited by R. K. Willardson and Albert C. Beer (Academic Press, New York, 1972), p.457.

20. J. Bardeen, F. J. Blatt and L. H. Hall, in Photoconductivity Conference, edited by R. G. Breckenridge, B. R. Russell and E. E. Hahn (Wiley, New York, 1956) p.146.

21. B. O. Seraphin and N. Bottka, Phys. Rev. 139, A560 (1965).

22. D. A. B. Miller, S. Des Smith, Colin T. Seaton, "Optical Bistability in Semiconductors", IEEE J. of Quantum Electronics, 17, 313 (1981).

23. D. S. Chemla, D. A. B. Millar, P. W. Smith, A. C. Gossard, W. Wiegmann, "Room Temperature Excitonic Nonlinear Absorption and Refraction in GaAs/AlGaAs Multiple Quantum Well Structures", IEEE J. of Quantum Electronics, 20, 265 (1984).

24. D. A. B. Millar, D. S. Chemla and T. C. Daman, A. C. Gossard, W. Wiegmann, T. M. Wood, "Novel Hybrid Optical Bistable Switch: The Quantum Well Self-Electro-Optic Effect Device", Appl. Phys. Lett. 45, 13 (1984).

25. Y. Hori, J. Paslaski, M. Yi and A. Yariv, "High-Speed InP Optoelectronic Switch with a Tandem Structure", to be published in Appl. Phys. Lett.

Table I

Material Parameters (Theoretical)

	Bandgap (eV)		Mobility at 300K (cm^2/v-s)		Effective Mass Ratio m*/m°		
	300K	0K	Elec.	Holes	Elec.	Holes	$\varepsilon_s/\varepsilon_o$
$In_{0.48}Al_{0.52}As$	0.73	0.82	$1.0x10^4$	200	0.034	0.4	12
InP	1.35	1.42	4600	150	0.077	0.64	14

Table II
Material Parameters (Experimental)

	Carrier Density (cm^{-3})		Hole Mobility (cm^2/v-s)		Thickness	Dopant	Growth
	300K	77K	300K	0K	(μm)		Temperature
$In_{0.48}Al_{0.52}As$	$6.6x10^{16}$		167		2	Zn	685°C
InP	$p > 10^7$ Ω-cm				~200	Fe	

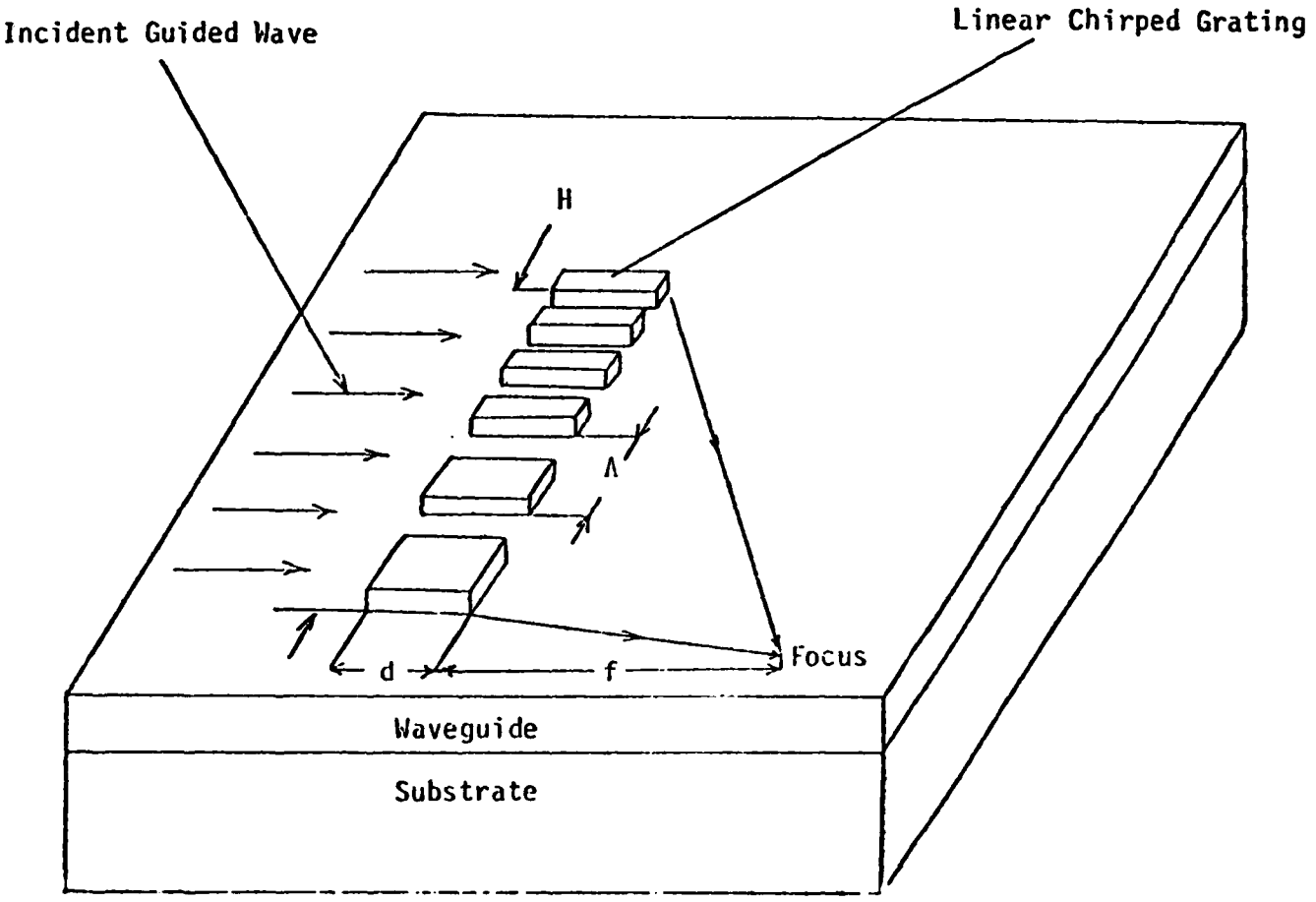

TYPICAL DIMENSIONS OF A GRATING LENS

d = (15 - 400 μm)

Λ = (1 - 20 μm)

H = (1 to several mm)

f = (5 - 30 mm)

Figure 1

Illustration of a Linearly Chirped Grating Lens

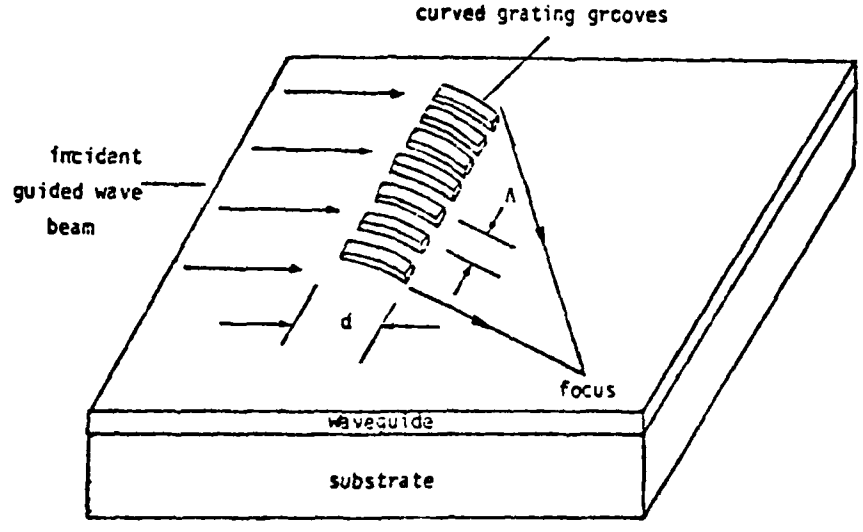

Figure 2 Illustration of a Curved Chirped Grating Lens

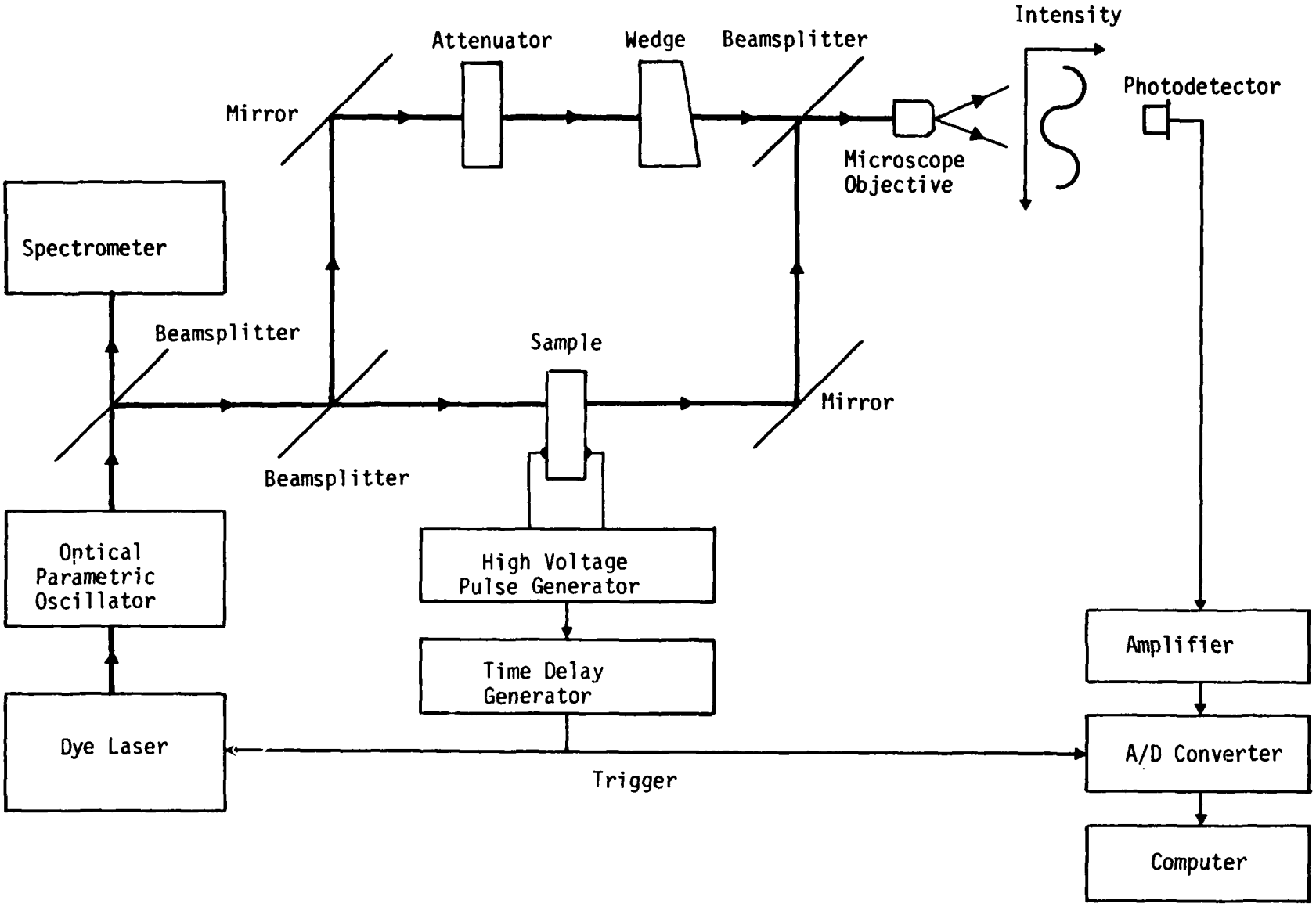

Figure 3 Schematic Illustration of the Electro-refraction Measurement

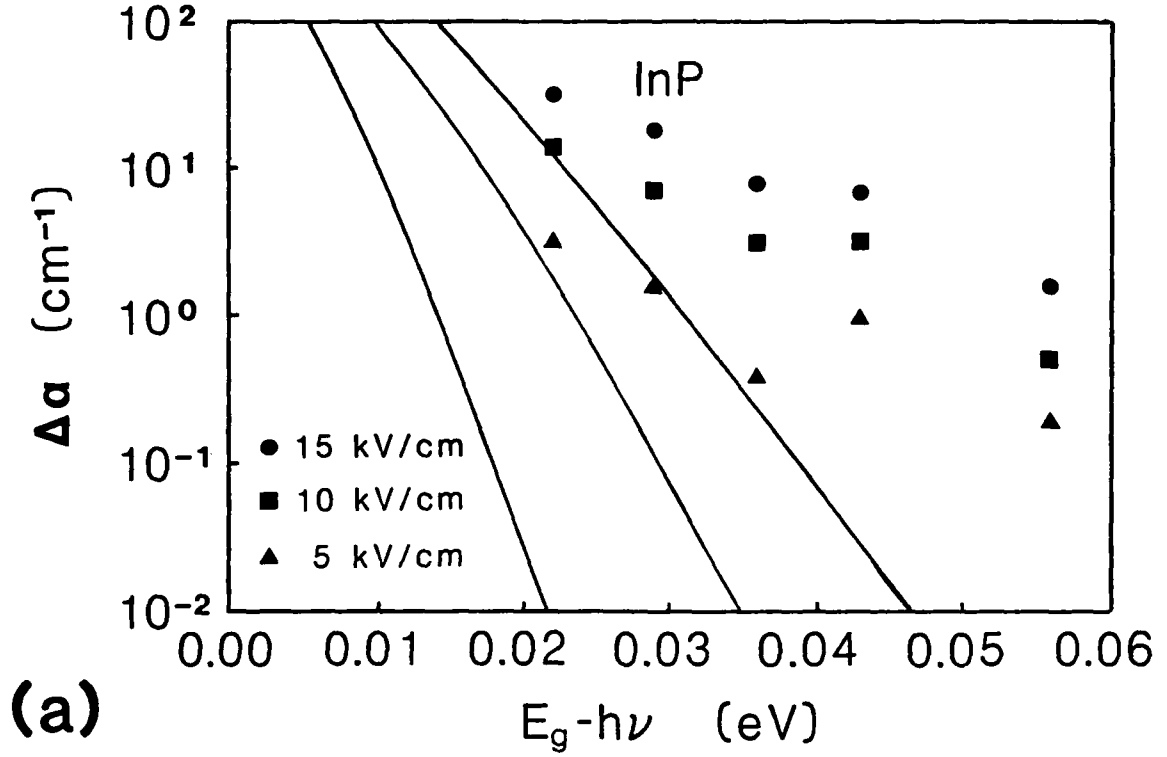

(a)

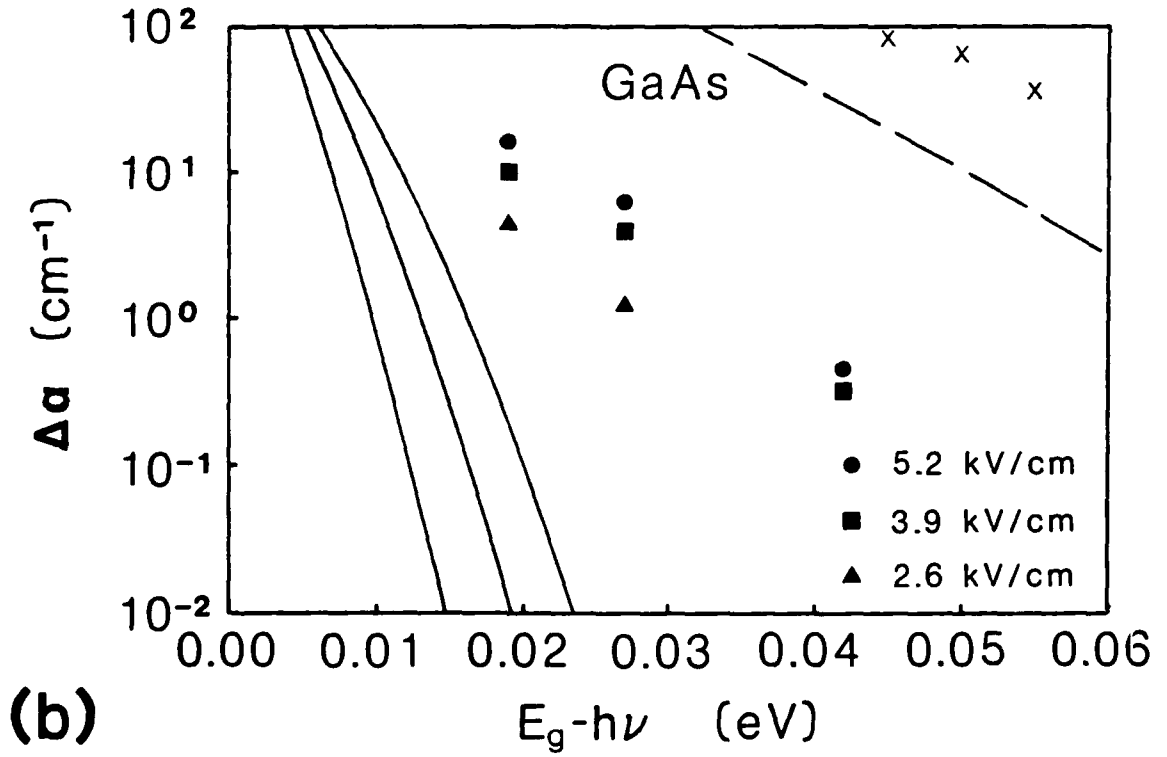

(b)

Figure 4 Electroabsorption in InP and GaAs

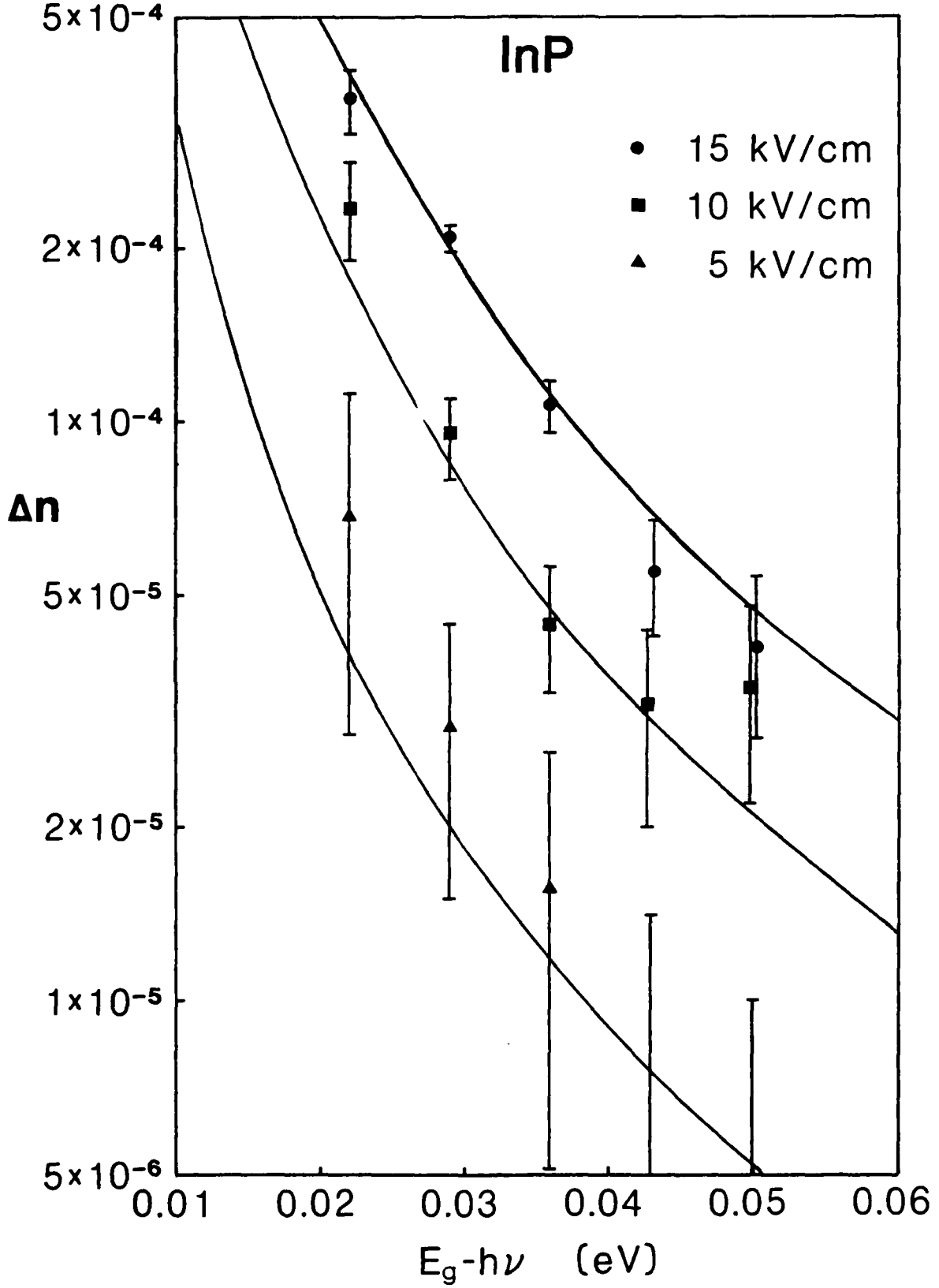

Figure 5 Electrorefraction in InP

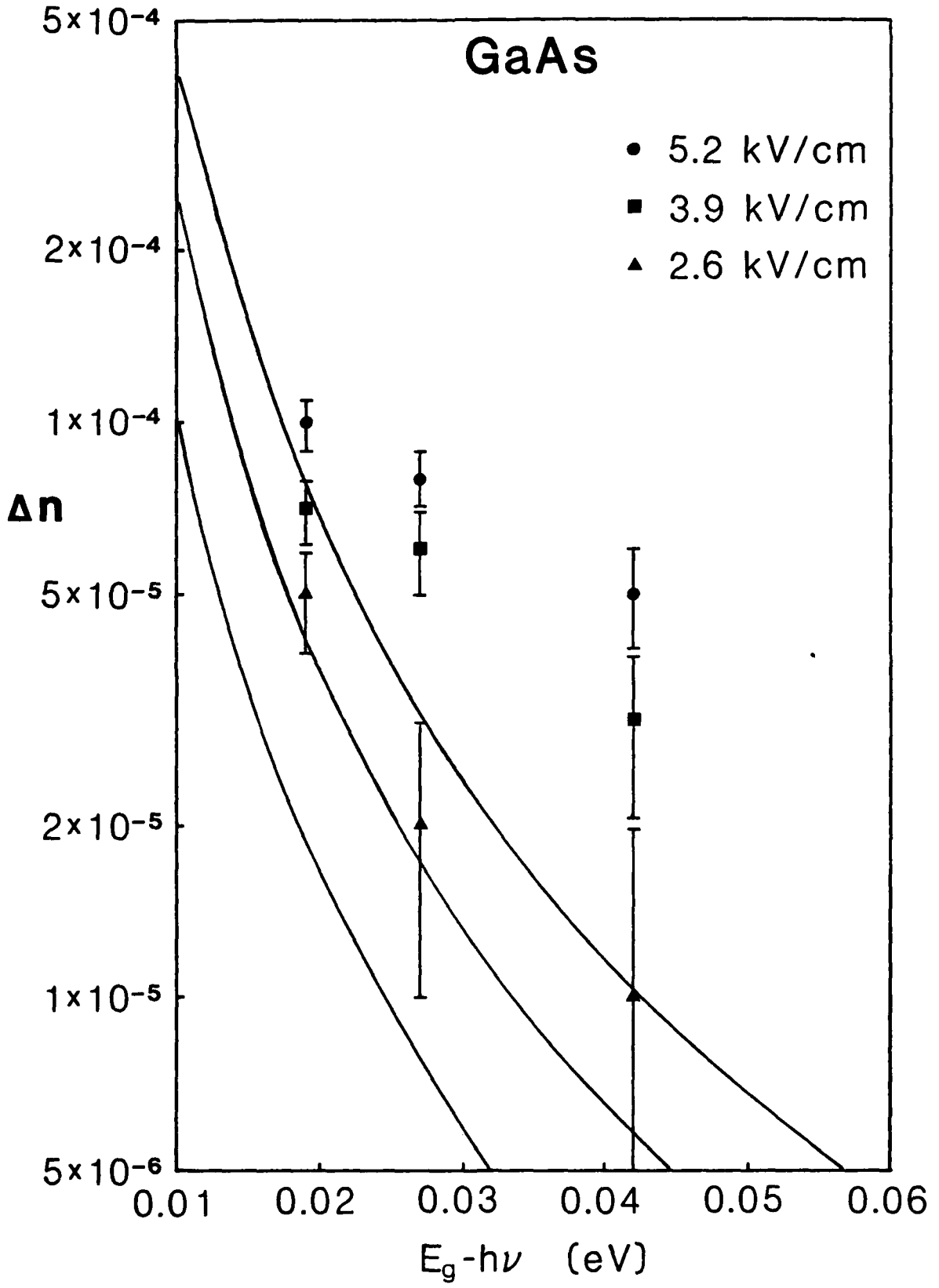

Figure 6 Electrorefraction in GaAs

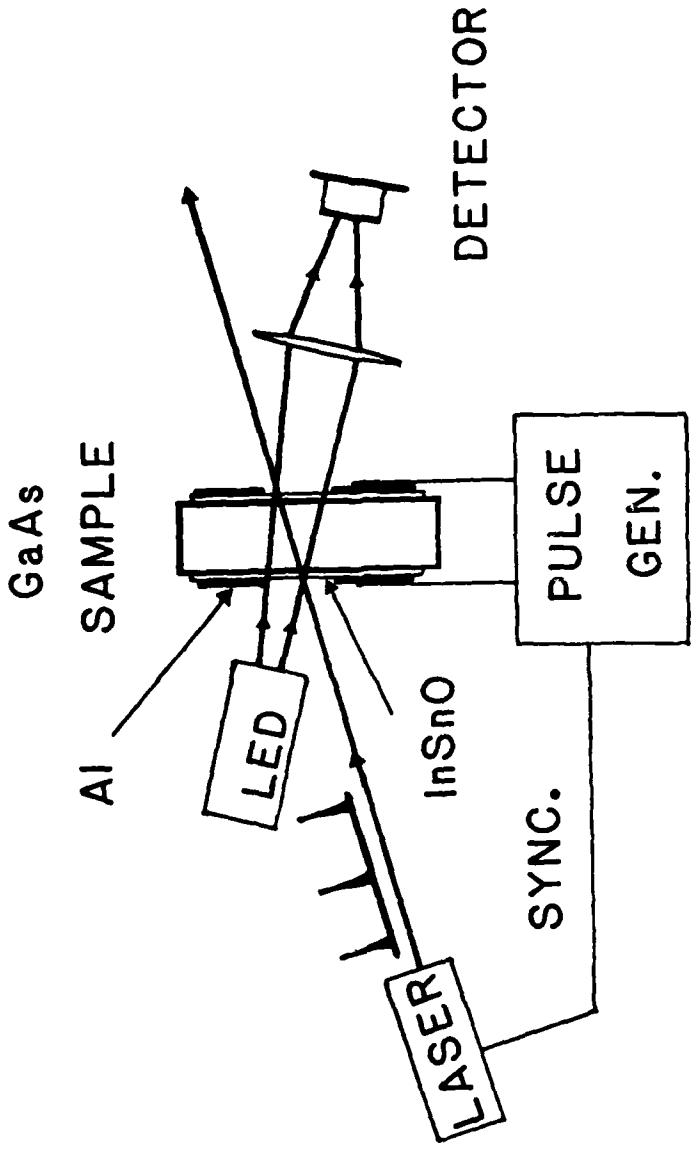

Figure 7 Schematic of the Cross Modulation Circuit

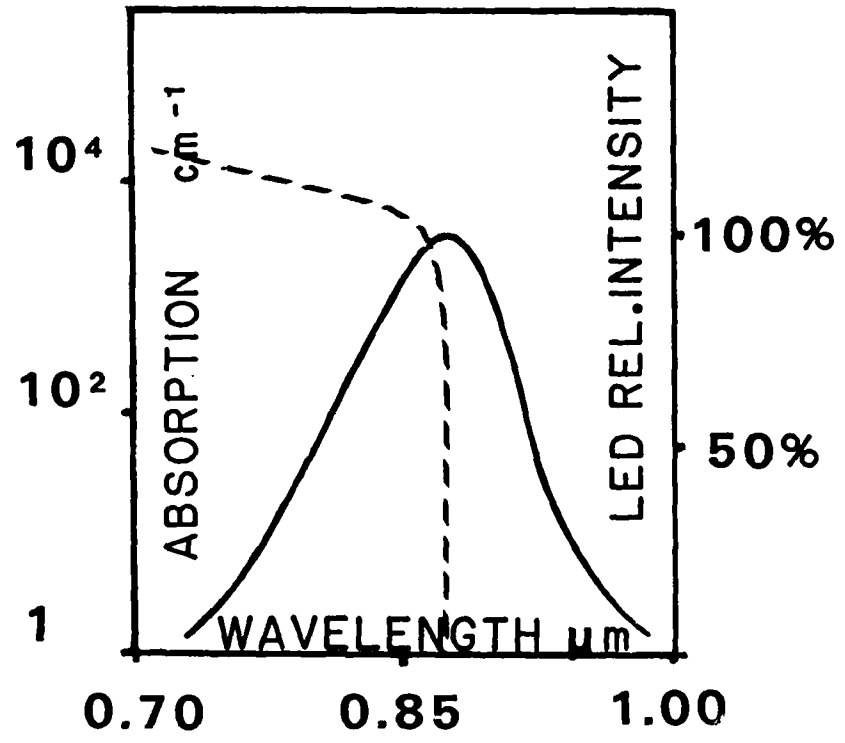

Figure 8 The wavelength spectrum of the LED in relation to the absorption edge of GaAs in the ideal situation is shown. The LED spectrum was obtained from the RCA data sheet.

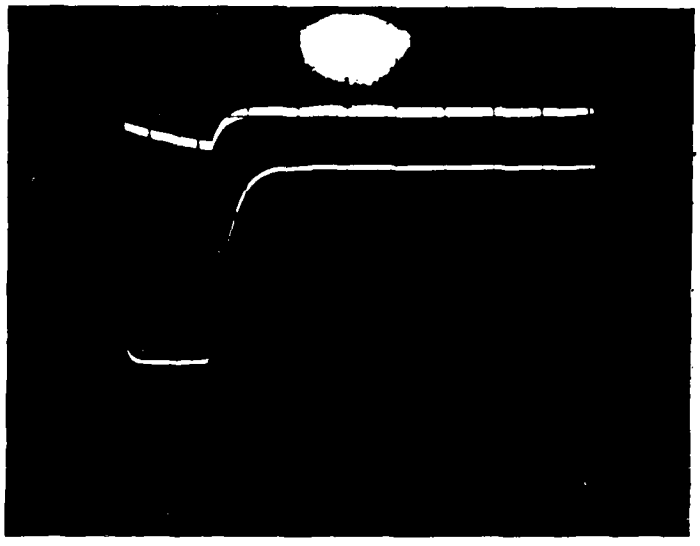

Figure 9 The absorption of LED caused by a voltage pulse is shown. The bottom trace is the voltage pulse with horizontal scale 15 μsec/cm and vertical scale 150 V/cm. The upper trace represents the absorption with vertical scale 10%/cm.

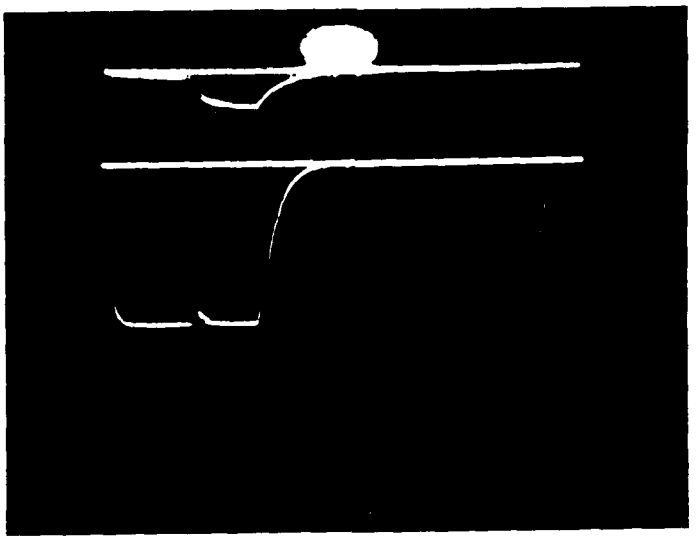

Figure 10 The effect of the optical pulse of 1 kwatt/cm^2 on the LED absorption is shown. The bottom trace is the voltage pulse with horizontal scale 15 μsec/cm and vertical scale 150 V/cm. The upper trace represents the enhanced absorption casued after the optical pulse, with vertical scale 75%/cm.

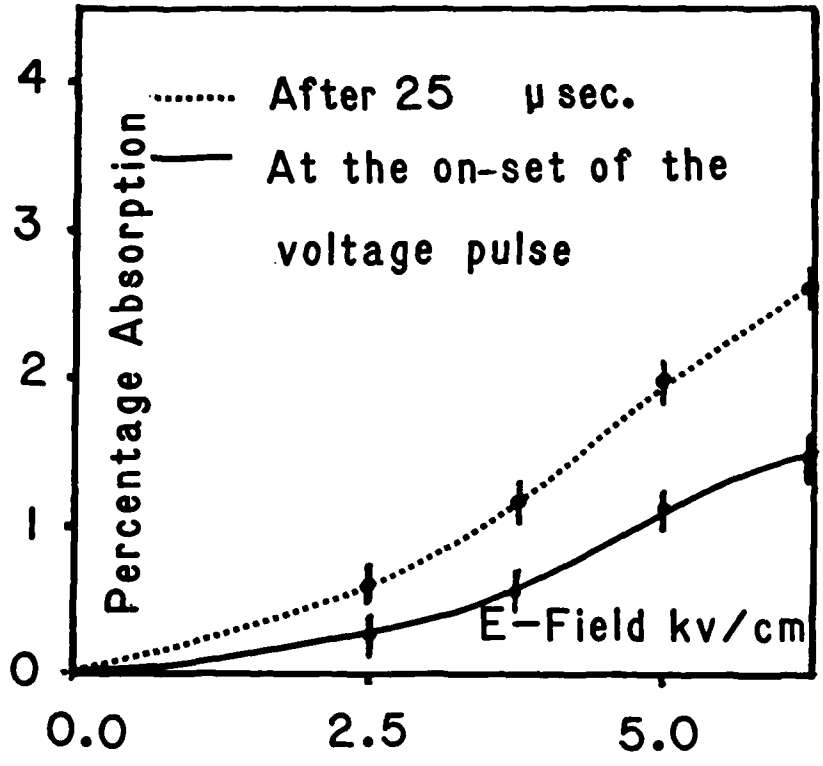

Figure 11 The absorption of LED light is plotted against the electric field caused by the voltage pulse:
a) at the onset of the voltage pulse,
b) after 25 μsec.

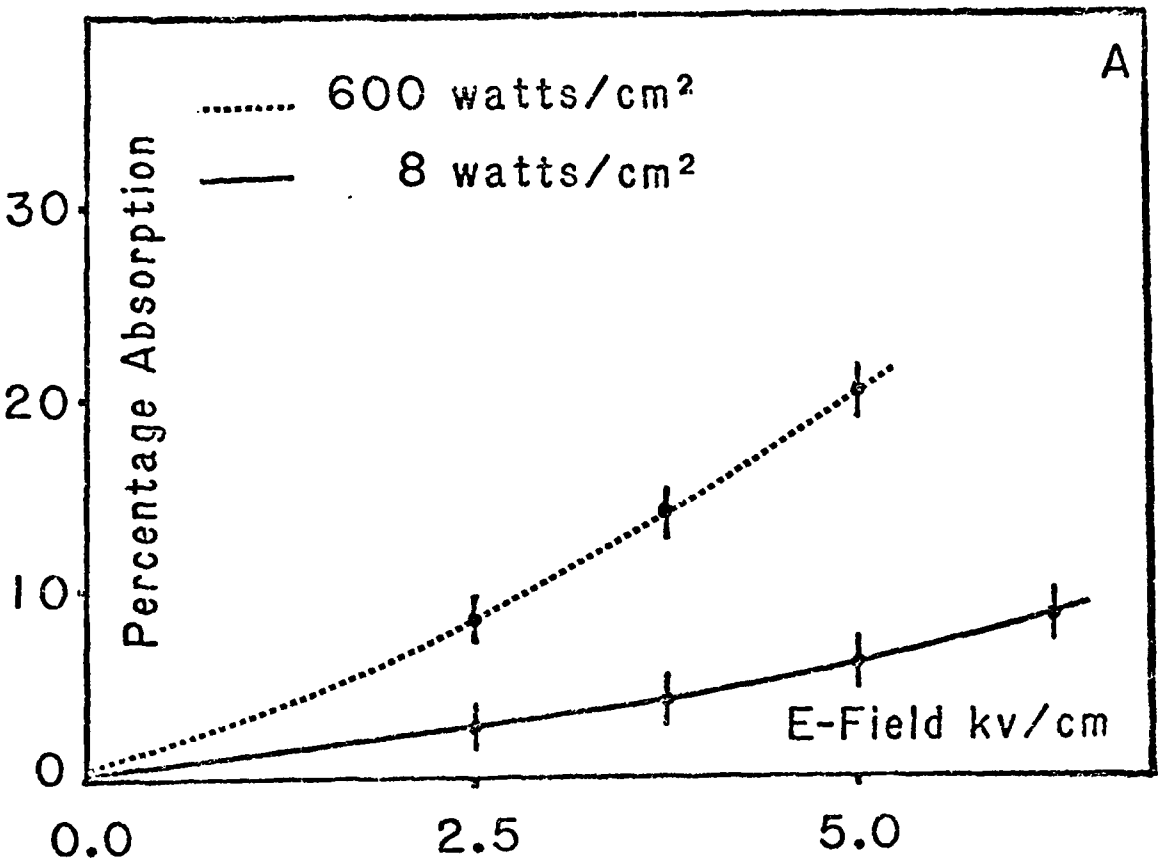

Figure 12 The enhanced absorption of the LED light after the optical pulse is plotted against the electric field.
a) optical pulse intensity 600 watts/cm^2.
b) optical pulse intensity 8 watts/cm^2.

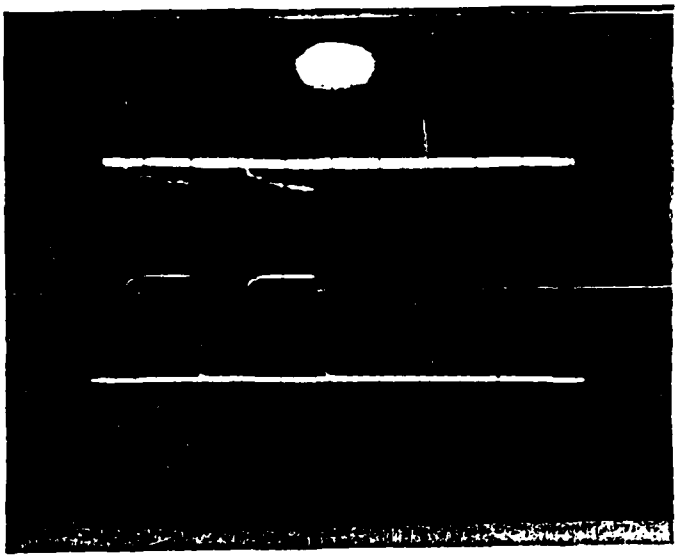

13a

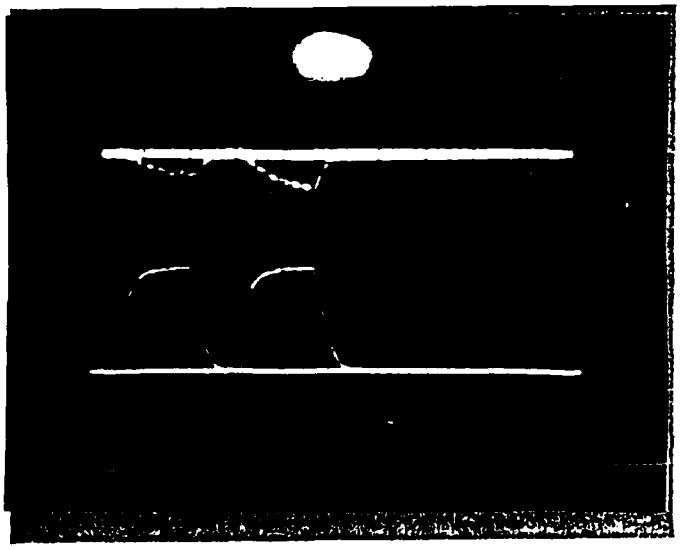

13b

Figure 13 The effect of an external RC time constant on the second voltage pulse is shown. The bottom trace is the voltage pulse with horizontal scale 30 μsec/cm and vertical scale 150 V/cm. The upper trace represents absorption with vertical scale 8%/cm.
a) No external capacitor across the sample.
b) With external capacitor (0.005 uF) across the sample.

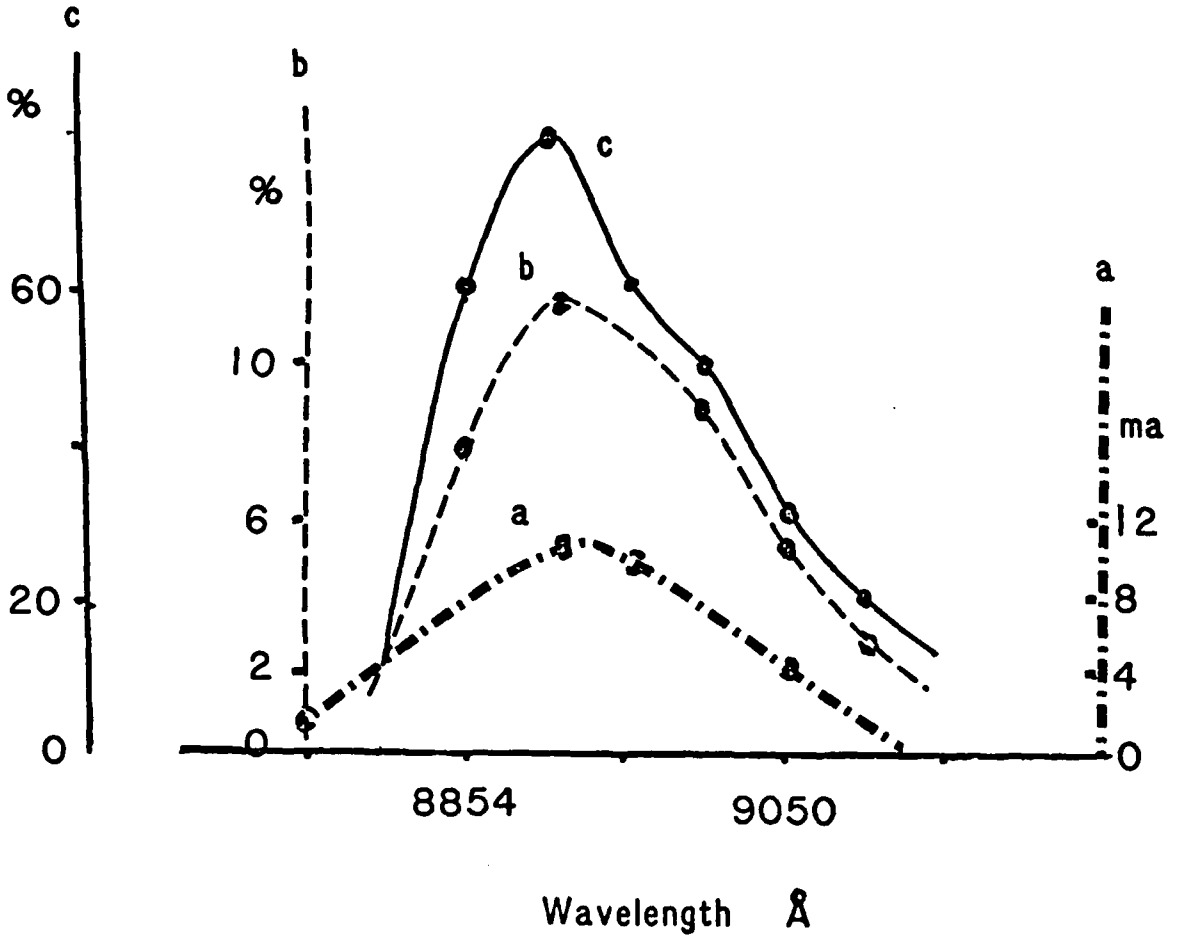

Figure 14 The effect of the optical pulse wavelength on the properties of the GaAs sample in the presence of transmitted LED light and applied pulse voltage is shown:

a) The current in the sample caused by the optical pulse is shown for voltage pulse 50 V and optical pulse intensity 6.3×10^{-7} Jouls/pulse.

b) The percentage absorption after the optical pulse is shown for voltage pulse 250 V and laser pulse intensity 6.7×10^{-7} Jouls/pulse.

c) The percentage reduction of voltage caused by the optical pulse generated current in the sample is shown. The applied voltage is 300 V and pulse laser intensity 1×10^{-4} Jouls/pulse.

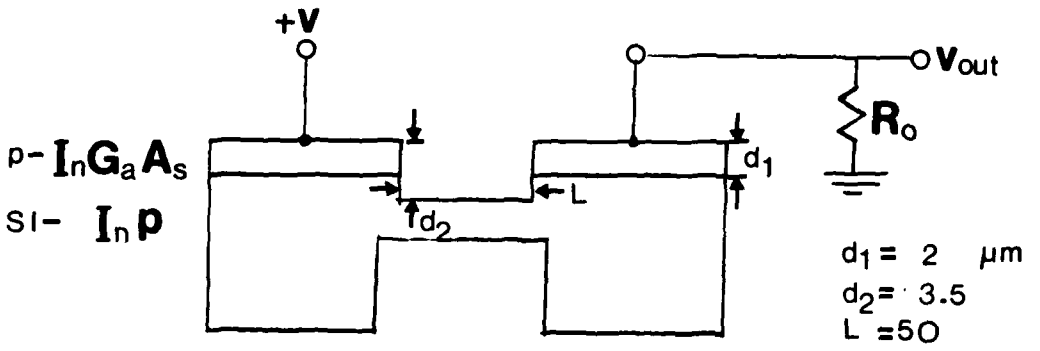

a.

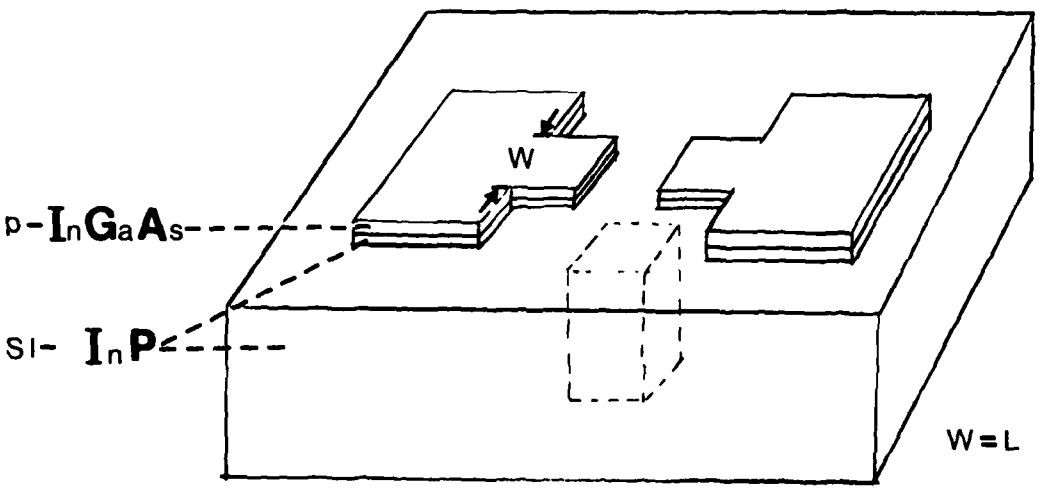

b.

FIG.15

The Photoconductor - photodiode AND gate

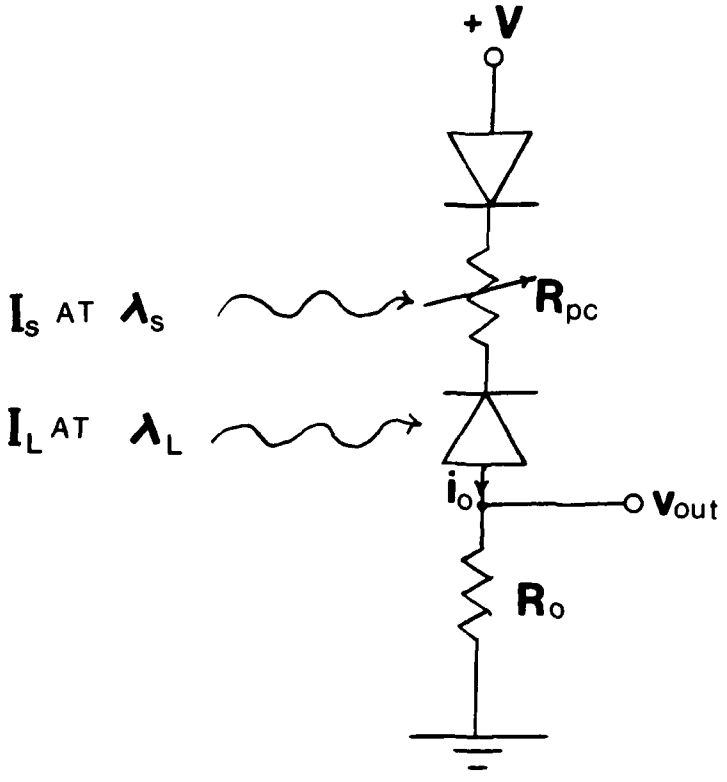

FIG.16

The Electrical Circuit Representation
of the Photoconductor - photodiode AN

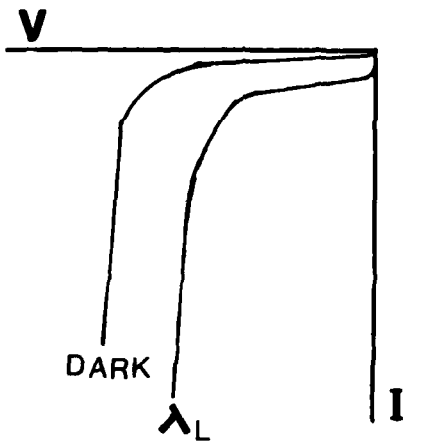

a. I–V CURVE OF PHOTODIODE

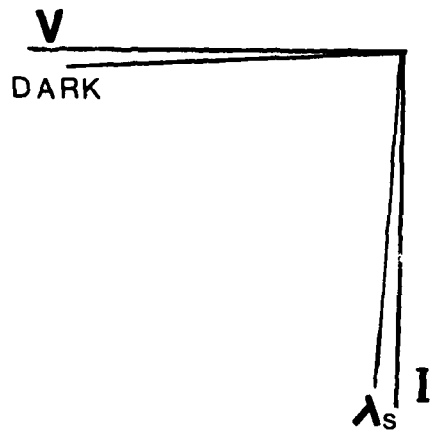

b. I–V CURVE OF PHOTOCONDUCTOR

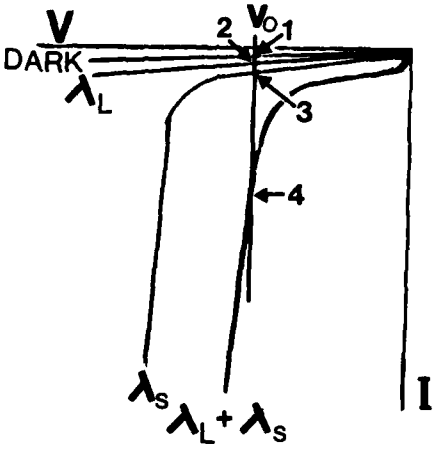

STATE	λ_L	λ_S	I_{out}
1	0	0	0
2	1	0	0
3	0	1	0
4	1	1	1

c. I–V CURVE OF **AND** GATE

FIG. 17

The I-V Characteristics of the AND Gate

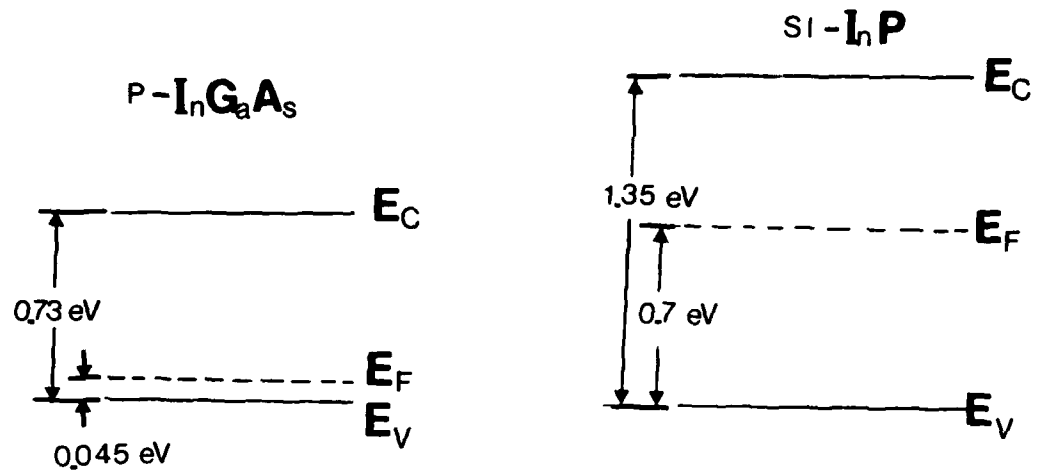

a.

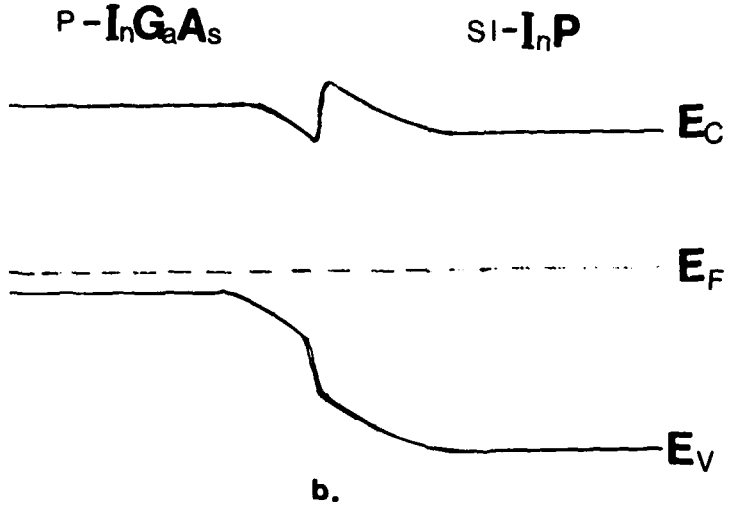

b.

FIG.18

The Energy Band Diagram of the InGaAs/InP Heterostructure

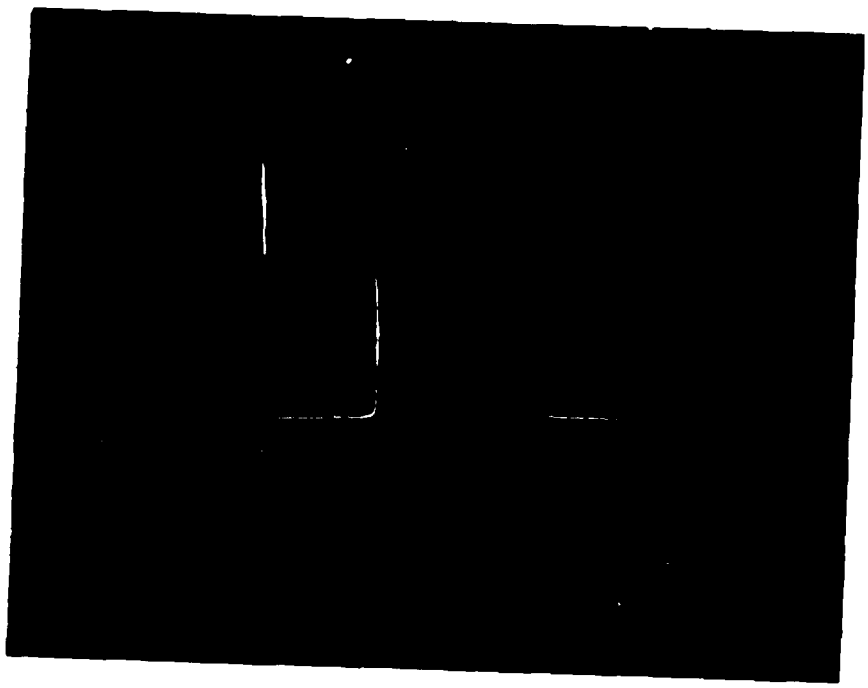

FIG.19 TOP VIEW OF THE **AND** GATE

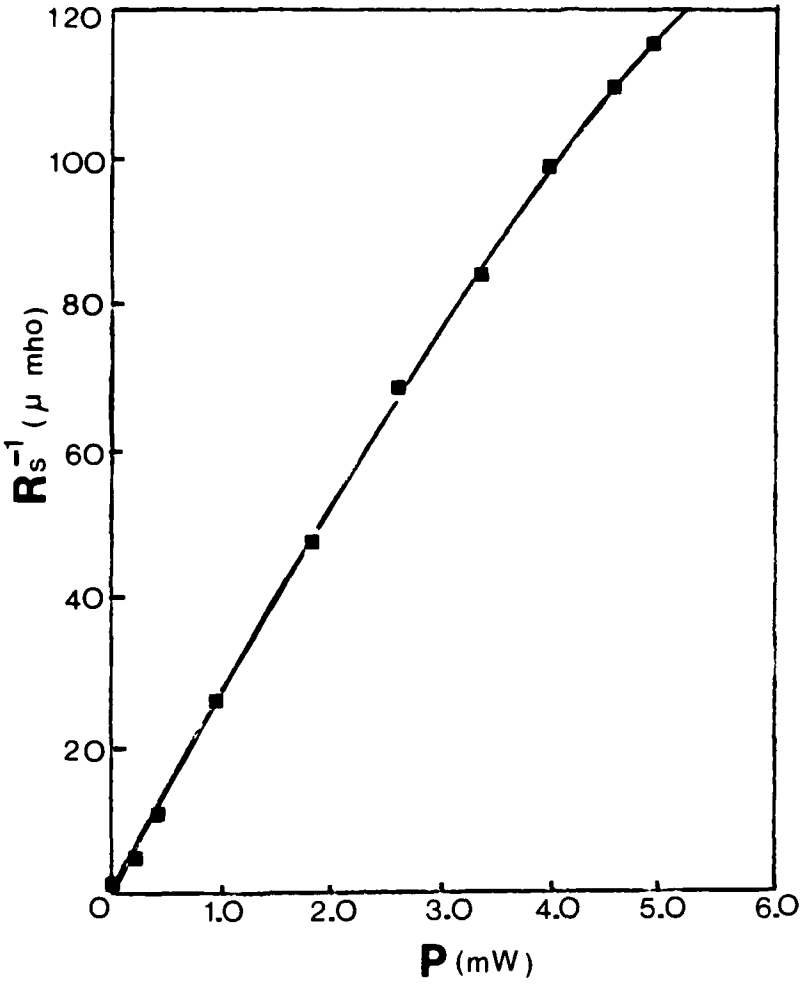

FIG.20

The Resistance of the InP Photoconductive Detector

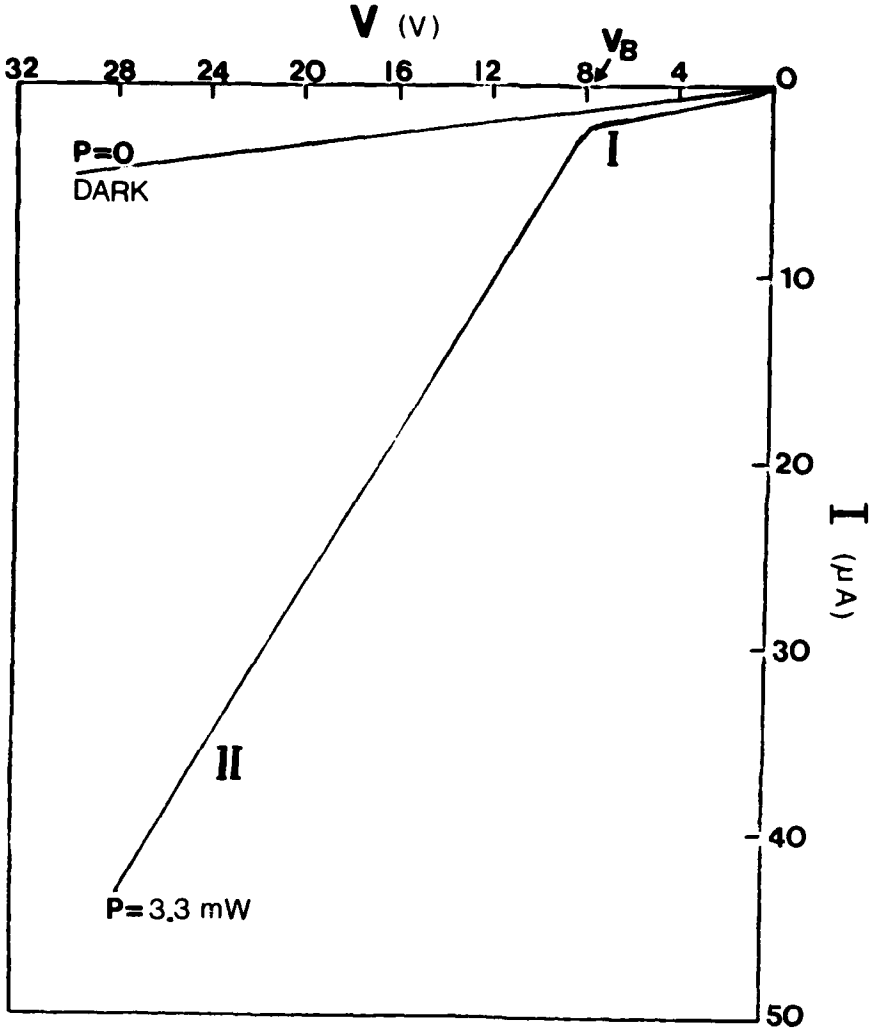

FIG. 21

The I-V Characteristics at 0.84 μm

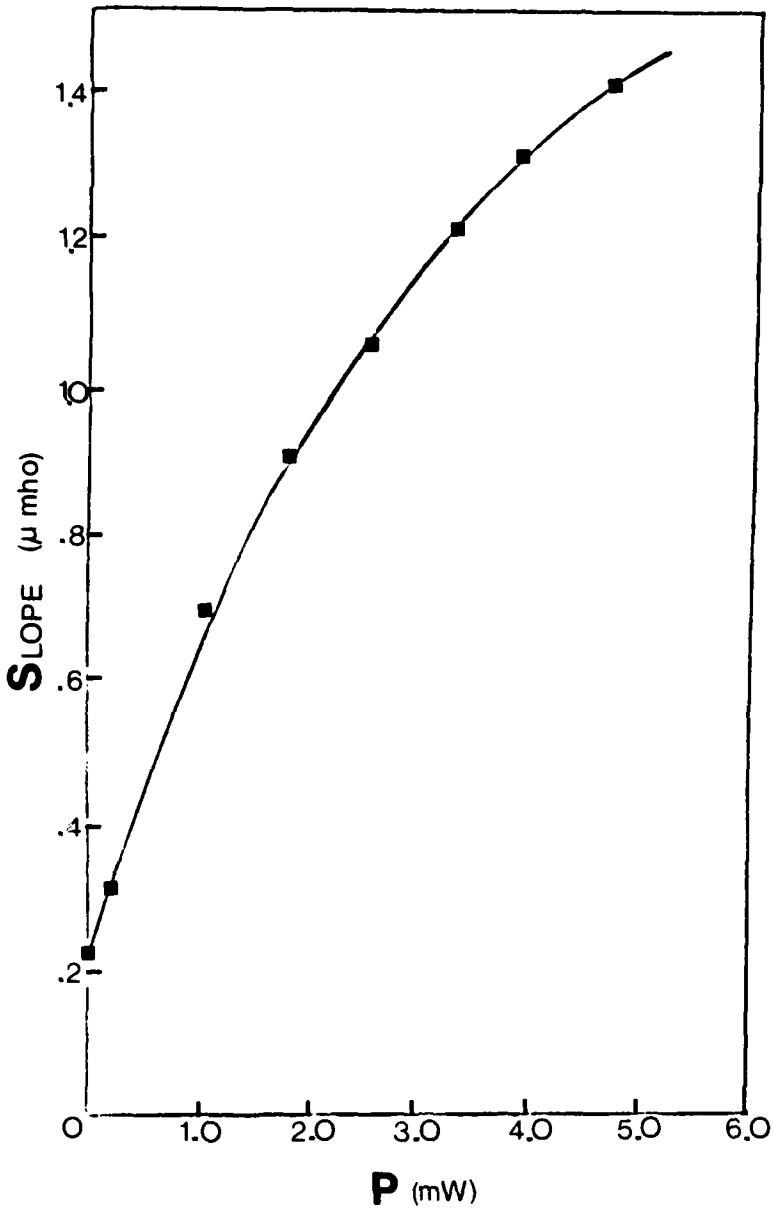

FIG.22

The Slope of the I-V Characteristics of the AND Gate at 0.84 μm Wavelength

END

FILMED

11-85

DTIC